2017-10-01

Evaluating the East Java Tsunami Hazard: What Can Newly-Discovered Imbricate Coastal Boulder Accumulations Near Pacitan and at Pantai Papuma, Indonesia Tell Us?

William Nile Meservy
Brigham Young University

Evaluating the East Java Tsunami Hazard: What Can Newly-Discovered Imbricate Coastal Boulder Accumulations Near Pacitan and at Pantai Papuma, Indonesia Tell Us?

William Nile Meservy

A thesis submitted to the faculty of
Brigham Young University
in partial fulfillment of the requirements for the degree of

Master of Science

Ron Harris, Chair
John McBride
Sam Hudson

Department of Geological Sciences

Brigham Young University

ABSTRACT

Evaluating the East Java Tsunami Hazard: What Can Newly-Discovered Imbricate Coastal Boulder Accumulations Near Pacitan and at Pantai Papuma, Indonesia Tell Us?

William Nile Meservy
Department of Geological Sciences, BYU
Master of Science

Our paleotsunami surveys of the southern Java coast led to the discovery of five imbricate coastal boulder fields near Pacitan, Indonesia that may date to the mid-to-late 19th century or prior and two similar fields at Pantai Papuma and Pantai Pasir Putih that were tsunami-emplaced during the 1994 7.9 Mw event in East Java. Estimated ages for the fields near Pacitan are based on historical records and radiocarbon analyses of coral boulders. The largest imbricated boulders in fields near Pacitan and in East Java are similar in size (approximately 3 m^3) and are primarily composed of platy beachrock dislodged from the intertidal platform during one or several unusually powerful wave impactions. Hydrodynamic wave height reconstructions of the accumulations near Pacitan indicate the boulders were likely tsunami rather than storm-wave emplaced, as the size of the storm waves needed to do so is not viable. We evaluate the boulders as an inverse problem, using their reconstructed wave heights and ComMIT tsunami modeling to suggest a minimum 8.4 Mw earthquake necessary to dislodge and emplace the largest boulders near Pacitan assuming they were all deposited during the same tsunami event and that the rupture source was located along the Java Trench south of Pacitan.

A combined analysis of historical records of Java earthquakes and plate motion measurements indicates a seismic gap with >25 m of slip deficit along the Java Trench. A 1000-1500 km rupture along the subduction interface of this segment is capable of producing a 9.0-9.3 Mw megathrust earthquake and a giant tsunami. However, evidence for past megathrust earthquake events along the this trench remains elusive. We use epicenter independent tsunami modelling to estimate wave heights and inundation along East Java in the event that the trench were to fully rupture. By translocating ComMIT slip parameters of Japan's 2011 9.1 Mw event along the trench offshore East Java, we demonstrate possible wave heights in excess of 20 m at various locations along its southern coasts. Approximately 300,00-500,000 people in low-lying coastal communities on the southern coasts of East Java could be directly affected. We recommend at-risk communities practice the "20/20/20 principle" of tsunami hazard awareness and evacuation.

Keywords: Tsunami, imbricate, boulder, earthquake, hazard, tsunami modelling, wave height, Java, Indonesia, Pacitan, East Java, beachrock, Bali, inundation, runup, Sunda, Java trench

ACKNOWLEDGEMENTS

This thesis has been an incredible opportunity, and special thanks is owed to so many people. In particular, I am indebted to my advisor, Dr. Ron Harris, who brought me to Indonesia and to a previously unknown love of studying natural hazards. Sam Hudson and John McBride assisted enormously both in preparing me for my summer of field research and in improving the manuscript. Many other professors and students from BYU, UVU, and UPN worked hand in hand with me in Pacitan to find and document these boulder fields. It was an amazing experience to get to know so many of them. Not enough good can be said of Bryce Berrett, who was especially instrumental in assisting with tsunami modelling, making inundation maps for Pacitan and East Java, and reviewing the manuscript.

Additionally, I am particularly grateful for Gilang Setiadi, Satrio Hapsoro, Wawan Boger, and everyone from BPBD Pacitan who worked side by side with me in discovering and documenting these boulders. I cannot say enough good things about all of these wonderful people, many of whom will remain lifelong friends. I think a piece of my heart will always remain in East Java. Terima kasih kepada semua teman saya dari Indonesia dan yang tinggal di Pacitan, khususnya mereka dari BPBD Pacitan.

Last, but certainly not least, I am grateful for the love and support of kind parents and in-laws that assisted our family by frequently babysitting our daughters while both my wife and I simultaneously pursued graduate degrees. Kristen, I could never have done it without you. I love you.

TABLE OF CONTENTS

LIST OF FIGURES

LIST OF TABLES

1. Introduction

Deadly mega-tsunamis that struck Sumatra and Japan in the 15 years brought renewed attention to the importance of evaluating tsunami hazards near seismic-susceptible, coastal communities. Much of this research in Indonesia has focused on Sumatra; however, Java and Bali may be as, or more, susceptible to the next megathrust earthquake and tsunami to hit Indonesia. We investigated the eastern part of Java for evidence of paleotsunami deposits to test whether megathrust earthquakes have happened in the past. We also make use of historical records of past earthquakes and tsunamis, inverse modelling of coastal boulder fields to determine wave heights, and ComMIT tsunami modelling of the possible Java Trench seismic gap to facilitate understanding of past tsunamigenic events and improve forecasting of potential tsunami hazards for Pacitan and East Java, Indonesia.

1.1 History of Tsunami Risk Near Pacitan, Indonesia

Historical accounts describe six localized tsunamis striking the southern coasts of Java over the last 430 years (Harris and Major 2016). Two of these are recorded as earthquake-induced flooding events that occurred in or around Pacitan, Indonesia during the mid-19th century:

"January 4, 1840 around 1:15 pm. Violent quake in Middle Java. In Patjitan (Pacitan) the first shocks were felt between 1 and 2 pm; the (shakings) lasted a good minute and were accompanied by a subterranean rumble. The walls of the houses received cracks. A flood wave followed the quake." (Wichmann 1918)

"October 20, 1859 around 5:30 pm. Patjitan, Patjitan Bureau, Madiun Province (East Java). Powerful shock accompanied by a flood wave. It occurred in the very moment that the ship "Ottolina" in the roadstead, Capt. J. J. PRANGE, was in the process on throwing out a TAU anchor. The rowboat performing this, loaded with anchor and chain, sank, and 11 of the 13 persons of the crew were able to be saved." (Wichmann 1922)

Several other powerful “subterranean rumbles” were also recorded around the mid to late 19th century in the vicinity of Pacitan, one of which was felt onboard a ship just offshore Pacitan. The longest in duration of these, and possibly most intense seismic event experienced in Pacitan’s modern history, happened January 30, 1840 and is purported to have lasted “nearly two minutes, exceed(ing) in intensity even …” the tsunami-producing event that had occurred near the start of that same month (Wichman 1918).

With the exception of Krakatoa's massive 1883 eruption, caldera collapse, and resulting tsunami (Hamzah et al. 2000), possibly the most widespread destructive tsunami event on record that Java experienced occurred in the late 16th century; however, the historical record is uncertain and primarily based on circumstantial evidence (Wichmann 1918; Harris and Major 2016). Highly destructive, but localized events, have also occurred more recently across Java within the last century. The largest of these were the 1994 7.9 Mw earthquake south of East Java and 2006 7.8 Mw earthquake south of Pangandaran in Central Java. Both produced tsunamis that killed hundreds in low-lying coastal communities along Java and Bali’s southern coasts (Polet and Thio 2003; Fritz et al. 2007). Seismic recordings from the last 100 years demonstrate that Java alternates between intervals of high and low rates of seismicity that vary over periods of 30-40 years (Hall et al. 2017), and may be transitioning into a new period of higher seismicity.

1.2 Evaluating Present Tsunami Risk

Java and Bali are located along one of the most active convergent plate boundaries on Earth. Due to unprecedented population growth, tsunami risk for these islands is greater today than ever before. In the last century alone, Indonesia’s population has increased nearly tenfold (Major et al. 2008). Today, approximately 4.35 million Indonesians reside in low-lying, coastal areas endangered by tsunamis along the southern coasts of Sumatra, Java, and Bali, and many of

these people may have as little as 20 minutes to escape to high ground in case of a tsunamigenic earthquake (Post et al. 2009). Of significant concern is a seismic gap (Fig. 1) along the highly active eastern segment of the Sunda Trench. This segment, known as the Java Trench, parallels Java, Bali, and other islands to the east. Historical records indicate that the Java Trench may not have produced a megathrust earthquake in over 430 years (Wichmann 1918 and 1922; Harris and Major 2016).

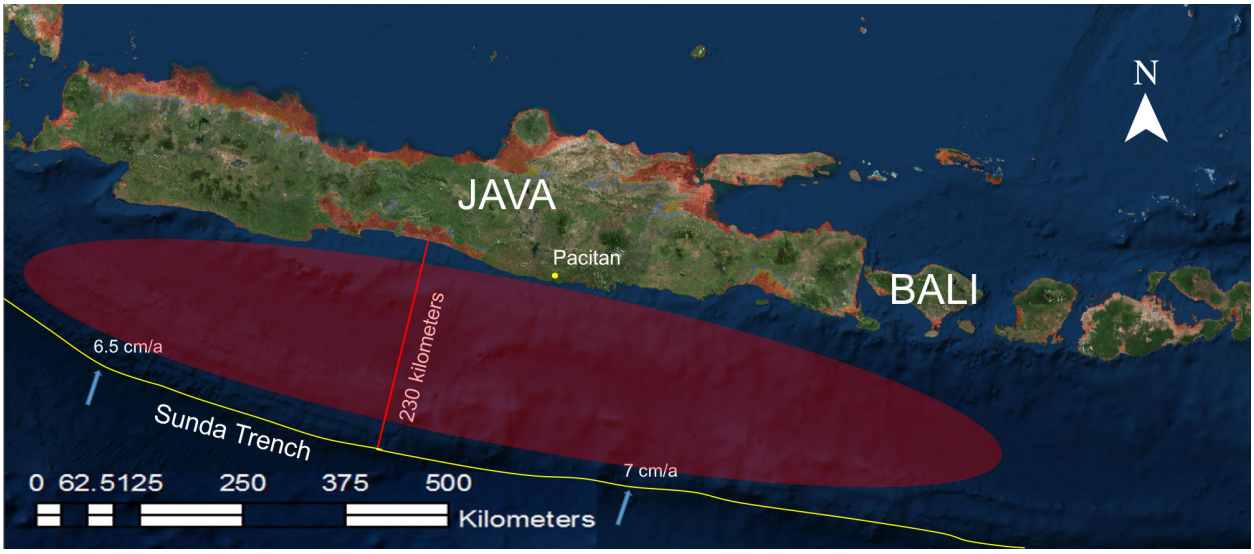

Figure 1. ArcGIS elevation map of Java and Bali. Red overlay on land shows topographic areas <30 meters above sea level. Tsunamis generated by earthquakes along the Java segment of the Sunda Trench (yellow line) typically reach the shore in about 30 minutes. Plate movement vectors in blue show plate converge faster to the east. In dark red, spherical overlay, a 1000 km seismic gap for the trench is approximated as a potential rupture area.

During this time, assuming the Java Trench is mostly locked and a steady 7 cm/a of convergence (Tregoning et al. 1994), an estimated 25 m of elastic strain may have accumulated along a >1000 km portion of the trench adjacent Java and Bali. This estimate includes slip released by known earthquakes along the convergent boundary over the past 430 years, which may have reduced the slip deficit along the subduction interface no more than 3 m. Elastic strain energy released from all currently known seismic events at the trench can explain only a limited

percentage of the cumulative total convergence at the plate boundary (Harris and Prasetyadi, 2002).

Empirical data compiled by Wells and Coppersmith (1984) provide a way to calculate the seismic moment (Mo) and moment magnitude (Mw) of a potential megathrust event along the Java Trench using the following relationships:

$$Mo = \mu * D * a$$

$$Mw = \frac{2}{3} * \log(Mo) - 10.7$$

Mo is calculated with μ as the typical shear modulus given for crustal faults at 3 * 10^11 dyne/cm^2, D as the average displacement along the fault at 25 m, and 'a' as the area of the fault at 1000 km * 144 km, which is estimated as the average width of the fault dipping at 10 degrees down to a 25 km depth. Accordingly, the Mw of a potential megathrust earthquake along the trench would be approximately 9.2-9.3 if it were to fully rupture. An event this size could trigger tsunami runup heights similar to megathrust events such as the 2004 Indian Ocean tsunami or the 2011 Japanese tsunami and would affect over 2 million people living in coastal communities along the south coast of Java, Bali, and other islands. Many of these communities have concave coastal topography that could amplify tsunami runup height and risk.

There are, however, several important questions about the seismic hazard along Java's offshore trench that still need further answering, including 1) whether the Java Trench is actually capable of producing megathrust earthquakes or whether it is limited to smaller, segmented events, 2) how much of the estimated accumulated strain energy may actually be accommodated by Java's back arc thrust system, 3) whether the trench may be mostly aseismic after all (Newcomb and McCann 1987), and 4) if megathrust earthquakes and tsunamis do occur along the trench, then do they have a consistent recurrence interval, or do they fluctuate from centuries

to millennia as in Sumatra (Rubin et al. 2017)? However, in the interest of building local resilience to potential earthquake and tsunami hazards, and without significant evidence confirming that the southern coastal populations along Java and Bali are not currently at risk of a mega tsunami, the offshore trench paralleling Java should be viewed as a major seismic gap and a significant safety concern.

1.3 Other Tsunami-Related Concerns

In addition to Java and Bali's worrisome offshore seismic gap, another tsunami-related concern that coastal populations face is a high risk of "tsunami earthquakes", a diagnostic term indicating a type of earthquake that produces an unusually strong tsunami relative to surface wave magnitude (Tsuboi 2000). Because tsunami earthquakes generate surface waves with longer periods and slower rupture velocities than typical tsunamigenic earthquakes, the tsunamis they produce are far more challenging to rapidly identify with current technology. As a result, there is considerable risk that those in harm's way will not be warned in time or at all. Hall et al. (2017) have developed and taught a "20/20/20 principle" that empowers individuals and discourages full dependence on tsunami early warning systems, which are prone to failure (Badan Meteorologi Klimatologi dan Geofisika 2010) or may cause fatal delays in evacuation (Lauterjung et al. 2010) of a potentially deadly tsunami. This educational tool can be easily taught and prepares at-risk locals by warning them that if an earthquake lasts longer than 20 seconds, even if it is hardly perceptible, those in low-lying regions have approximately 20 minutes to evacuate to a height of 20 meters or more if possible.

Both the deadly 1994 and 2006 tsunamigenic earthquakes affecting Java were deemed tsunami earthquakes (Synolakis et al. 1995; Ammon, Kanamori, and Velasco 2006) and were hardly felt, even though the shaking was prolonged. The trench adjacent to Java and Bali may be

more prone to these kinds of slow-rupture earthquakes for a variety of reasons, including regional fault slip barriers, asperities, and other topographic heterogeneities in the subducting slab (Bilek and Engdahl 2007). Substantial crustal deformity near the trench is thought to be related to the subduction of Roo Rise (Fig. 2), an oceanic plateau off East Java that has heavily altered the nearby accretionary prism, adding to the challenges scientists face in assessing local tsunamigenic earthquake risks (Shulgin et al. 2011).

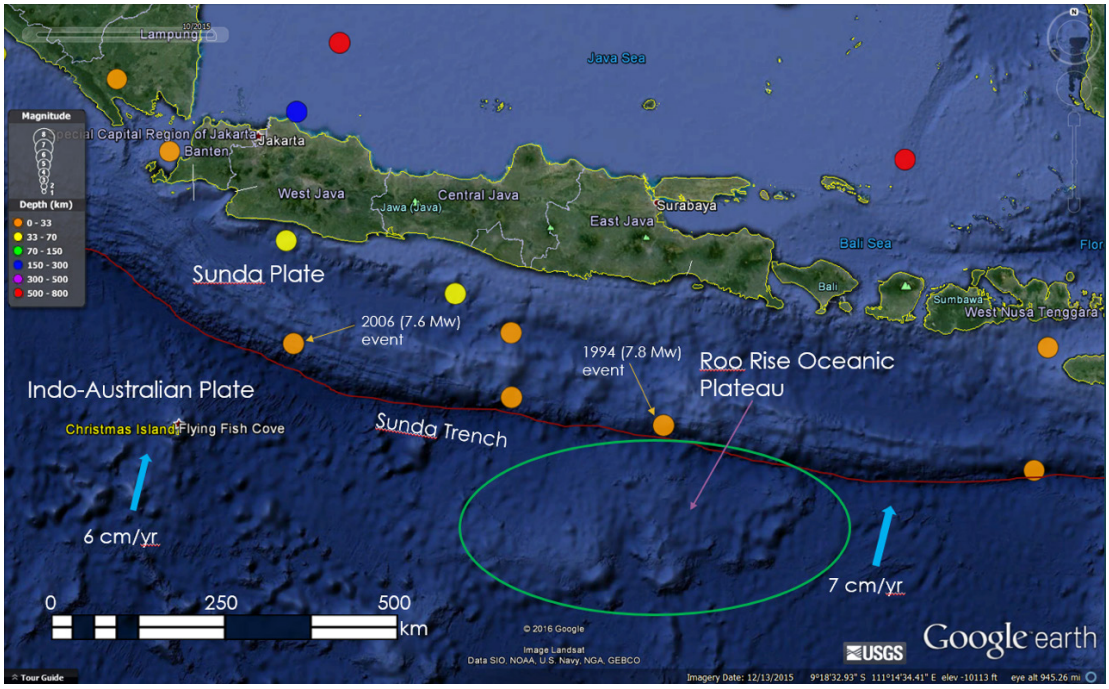

Figure 2. Google Earth map of Java, Bali, and the eastern portion of the Sunda trench with plate vectors and every major earthquake (7.0-7.9 Mw) recorded by the USGS since 1900. The largest event, a 7.9 Mw, is not enough to have majorly impacted currently accumulated slip. Roo Rise is visible in the bottom right corner.

The subduction of Roo Rise also contributes to frontal erosion of the accretionary wedge (Kopp et al. 2006; Brune et al. 2009), a process at some convergent margins that may be linked to an increased risk of coseismic, submarine landslide-induced tsunamis (Harders et al. 2011). Submarine landslides are infrequent and, therefore, difficult to forecast (Masson et al. 2006). However, depending on their location, they can trigger localized tsunamis with extreme runup

heights (Harbitz et al. 2014), which are capable of reaching the shore in far less time than most tsunamigenic earthquake modelling predicts.

2. Imbricate Boulder Accumulations

2.1 Surveying for Paleotsunami Evidence in Java

Although historical records provide accounts of smaller tsunamis hitting Java's southern coasts, much of their corresponding geologic footprint is not well preserved, or at least has proven challenging to find. Unlike many other recent, tsunami-deposited sand sheets across the globe, evidence of large tsunamis in Java are difficult to find due to poor preservation and cultivation. For example, evidence of Krakatoa's massive 1883 tsunami, which produced 37 m high waves and killed over 36,000 people in West Java, is difficult to locate. According to Paris et al. (2014), "the 1883 tsunami...deposits are not preserved everywhere, and are often reworked through bioturbation, slope processes, fish farming, tourist resorts, agriculture, and industries." Java is the most densely-populated, large island on Earth and is agronomically-dominated from coast to coast; thus, there are very few areas along its southern coasts that have not historically and recently been altered by humans for agricultural purposes or by other forms of rapid bioturbation.

Java is also one of world's wettest islands located along a convergent plate boundary. Because of this, trenching efforts to survey for paleotsunami deposits are often hampered by Java's high level of groundwater saturation, and Java's many rivers may also contribute to rapid erosion of sand sheets. Atwater (2007) argues that paleotsunami recorders may prove harder to find in wetter areas around the Indian Ocean like Java than in more temperate but otherwise similar settings along the Pacific Rim because of disturbances to the deposits by crabs and farmers. He suggests that, "the reasons for this challenge are probably unrelated to tsunami size

or recurrence." Several recent attempts across the entire south coast of Java by LIPI in collaboration with BYU, UVU, and UPN to locate paleotsunami sand sheets in swales within a half kilometer of the coast have yielded only a few tsunami sand layers that date back to around 1600 AD.

However, some surveying techniques in densely-populated, tropical climates like Java have thus far proven more effective. When surveying for onshore, overwash tsunami deposits in Java, it is probably most effective to seek out places where the geologic record is least likely to be removed. Low-lying, coastal caves and lagoons may provide the best onshore topographic traps for paleotsunami sand deposition because their underlying stratigraphy is less likely to be disturbed (Rubin et al. 2017) by agriculture. Another onshore alternative is to survey along the coast for ridges, or fields, of imbricated boulders (Fig. 3), which provide good markers of high-energy events (Nandasena et al. 2010). Java, Bali, and other islands adjacent the eastern Sunda trench are particularly good environments for surveying for coastal boulder fields because major storms are less common than tsunamis at the equatorial location just south of the typhoon belt and north of the cyclone belt.

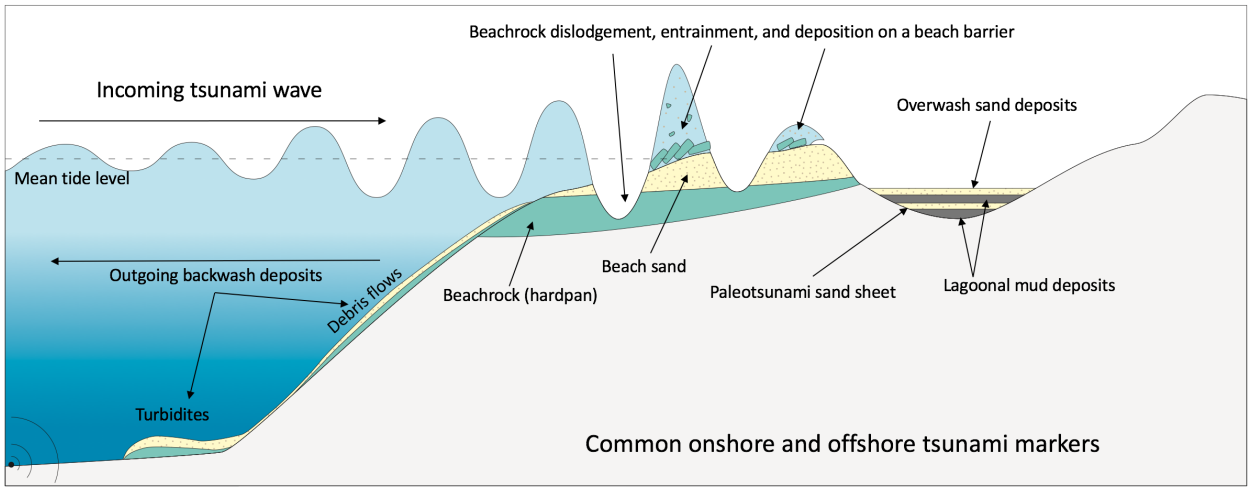

Figure 3. Common overwash and backwash deposits produced by tsunami. In a humid, coastal environment like Java, imbricate boulder accumulations may be the most resilient onshore tsunami marker because they are less likely to be perturbed by bioturbation or storm waves.

Ultimately, answering the question of whether Java's offshore trench is actually capable of producing megathrust earthquakes and tsunamis may require many different onshore exploration methods and should additionally include searching offshore for shallow marine, backwash deposits in the form of debris flows or turbidites. As of yet, however, little work in this latter regard has been accomplished along Java's southern coasts. Additionally, unlike Sumatra, offshore Java has no visible microatolls that can be sampled to build a detailed chronology of seismic deformation along the coast (Philibosian et al. 2017).

2.2 Coastal Boulder Field Locations and Compositions

An expedition in May 2016 to Pantai Papuma (Fig. 4), a beach that was affected by the 1994 7.9 Mw earthquake and tsunami in Java, discovered well preserved imbricated boulder accumulations composed of slabs of beachrock. This deposit (Fig. 5), and another to the east at Pantai Pasir Putih, were not recognized during post-tsunami surveys (Marami and Tinti 1997; Synolakis et al. 1995; Tsuji et al. 1995), and are described here for the first time. Local Javanese fishermen, who witnessed the tsunami at Pantai Papuma, independently provided firsthand accounts of changes to the coastline that occurred, each stating their belief that the boulders were deposited by the tsunami, and that the beaches had no apparent boulder ridges before the 1994 event. This lack of observable boulder ridges before the 1994 tsunami is difficult to interpret in light of the high probability of recurring events, especially considering large beachrock imbrications now dominate much of Pantai Papuma's coastline. Explanations for this ostensible anomaly include the possibility that boulders from any previous tsunamis were buried by sediment over time or that previous ridges had degraded so substantially that they were beyond easy recognition.

The eastern-most beach, Pantai Pasir Putih, which is in a nationally protected forest and difficult to access, translates to “White Sand Beach”. However, after the 1994 tsunami all of the sand was removed and the beach is now entirely covered by imbricated boulders and cobbles that spill several meters back into the forest, partially obscuring the base of some trees. It is possible that the tsunami removed the sand that was covering older boulders as well as new ones.

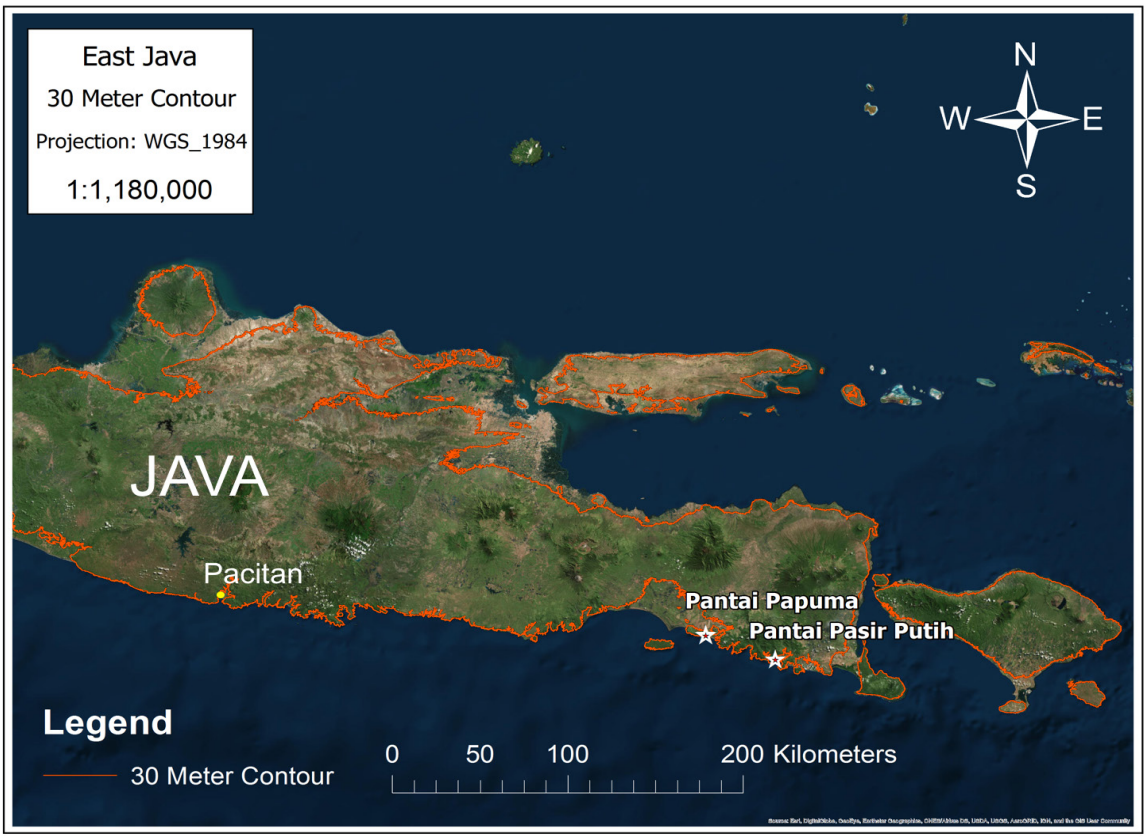

Figure 4. ArcGIS image of East Java, Indonesia and starred locations of coastal boulder fields emplaced during the 1994 7.9 Mw earthquake and tsunami. The orange line is at 30 m elevation. Pacitan is at the western edge of what is considered East Java.

Figure 5. Coastal boulder imbrications at Pantai Papuma (left and top left) and Pantai Pasir Putih (bottom right) in East Java.

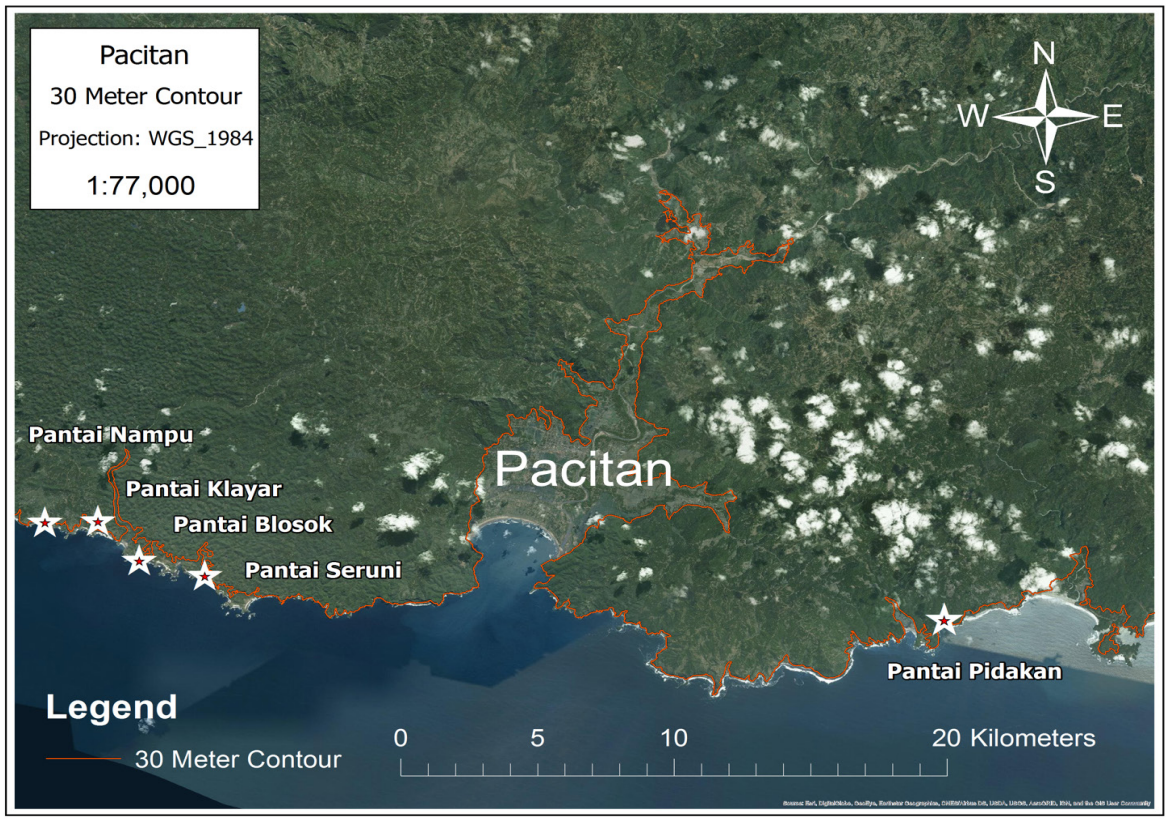

Figure 6. ArcGIS image of Pacitan, Indonesia and starred locations of five newly-discovered coastal boulder fields to the west and the east of Pacitan. The orange line is at 30 m elevation. Most of Pacitan is below this and susceptible to possible inundation by a major tsunami.

In July of 2016, we discovered five imbricate coastal boulder fields (Fig. 6) at beach locations near Pacitan that have not been previously described. Four of these (Fig. 7), Pantai Nampu, Pantai Blosok, Pantai Klayar, and Pantai Seruni, are located just to the west of Pacitan, with the farthest roughly 16 km away. Another of the fields, Pantai Pidakan (Fig. 8), is strewn across a kilometer-long stretch of beach approximately 15 km to the east of Pacitan. All of the beaches on both sides of Pacitan were partially covered in sand, differing in this regard from the beaches in East Java. Each field varies in length and width, the longest and widest to the west being Pantai Blosok with a length of 87 m and a width of roughly 8 m. On the east side of Pacitan, Pantai Pidakan stretches over 100 m in length but is far narrower, averaging only a few m in length at any given point. Of all the beaches in East Java and near Pacitan that we observed, Pantai Papuma has the longest boulder ridge at over 200 m in length and averaging approximately 8 m in width.

Figure 7. Coastal boulder imbrications west of Pacitan. Clockwise from top left: Pantai Nampu, Pantai Blosok, Pantai Seruni, and Pantai Klayar.

Figure 8. Coastal boulder accumulations at Pantai Pidakan, east of Pacitan. Larger, platy, beachrock boulders are deposited directly on top of smaller limestone boulders.

Almost all of the imbricate boulder fields we examined are comprised of a form of dense, calcareous sandstone, or beachrock (hardpan), that commonly forms the surface of the intertidal platform just offshore Java. The compositional exceptions are the accumulations at Pantai Nampu, which includes several limestone and sandstone boulders that may be sourced from prominent cliffs behind the beach, and at Pantai Pasir Putih, which is entirely covered with limestone boulders that can be sourced from nearby cliffs, and which are relatively smaller and rounder than the boulders located at any of the other fields. At every other beach besides Pantai Pasir Putih, nearly all of the boulders are thin, platy beachrock whose shortest axes average around 0.25 m long. Volumes of the largest boulders range between 0.3 to 3 cubic m.

As is common with accumulations of tsunami-deposited boulder imbrications, none of the boulders observed were transported great distances inland (Etiennes et al. 2011), and all of the fields are located near the shoreline and their source location. The largest boulders entrained in a high energy wave are normally dragged rather than suspended or saltated and, therefore, strongly affected by the friction of the underlying surface they are transported across. There is erosional drag evidence that some boulders travelled >200 m across the intertidal platform before making landfall and accumulating as a beach deposit. In addition, prominent excavations across the intertidal platform directly in front of the rest of the fields, and including Pantai Nampu to some extent, support the hypothesis that many, if not all of the boulders were ripped, or plucked, from offshore joint bound platforms during one or several large wave impaction events. Conversely, widespread excavations along the intertidal platform are not observed along adjacent sections of the intertidal platform directly in front of shoreline where there are no boulders found (Figure 9).

Figure 9. (Left) boulder dislodged and dragged over 200 m across the carbonate platform in front of Pantai Blosok. (Right) Boulder ridge at Pantai Blosok. The carbonate platform directly in front of the beach deposit, and only in front of it, is visibly stripped of all beachrock. Waves at Pantai Blosok normally break >200 m offshore and are said by locals to never pass beyond the mangrove trees just behind the boulders even during the annual highest tides.

2.3 Directional Statistical Analyses

The ocean's surface runs virtually unimpeded from Antarctica to the southern shores of Java, a distance that facilitates the regular development of unusually high waves to form and break along its coasts. These large waves, especially at high tides, contribute to significant coastal erosion in the region, and evidence of rapid undercutting and recent cliff failure is visible throughout much of East Java's continuously changing southern coastline. Typically, when a coastal cliff collapses, or a landslide occurs near the coast, rocks are distributed randomly along the coastal bench and produce no or very little preferred orientation. However, when a wave excavates beachrock from the seafloor, transports it inland, and deposits it in an imbricated boulder accumulation along the coast, the slabs or rock exhibit a preferred strike parallel to the wave which deposited them (Figure 10). Exceptions may include some movement and redistribution of slabs altered by a storm or another tsunami (Felton and Crook 2003). The offshore, underwater topography dictates that this orientation will commonly be along strike with the beach. In addition, rockfalls forming from the collapse of a coastal cliff or from a landslide

are typically far more rounded than boulders plucked from the seafloor, which are typically rectilinear in the strike direction (Figure 11).

Figure 10. Google Earth image of GPS coordinates for all boulder strikes (recorded with FieldMove Clino) at Pantai Blosok. The mean trend is about 120 degrees.

Strikes were taken of a large number of imbricated boulders at each beach visited in order to determine the overall preferred orientation. The mean orientation was calculated and the distribution of strikes for each beach is visualized in the rose diagrams below (Figure 12). Additionally, a Rayleigh test for circular uniformity for each boulder field was computed in MatLAB, demonstrating that the overall distribution of each sampled data set around a circle is not uniform, or not random. Since each imbricated boulder field we sampled exhibits a nonrandom distribution, we conclude that they were all wave-deposited, even those boulders at Pantai Nampu that were not composed of beachrock, and not deposited directly by collapse of a coastal cliff or landslide. No boulders at Pantai Pasir Putih were directly measured, as we did not receive governmental authorization to conduct research there and were only permitted to photograph the boulders.

Figure 11. Pictures of Pantai Blosok: (Left) Several layers of imbricated, platy boulders. White pen for scale. (Center) Excavations from the carbonate platform are visible at lowtide. (Right) A warung, or Indonesian eatery, is located just a few meters in back of the boulder field. Its owner says that the ocean never reaches the trees in front of it.

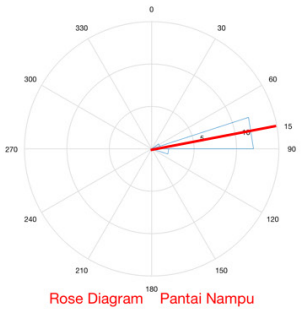

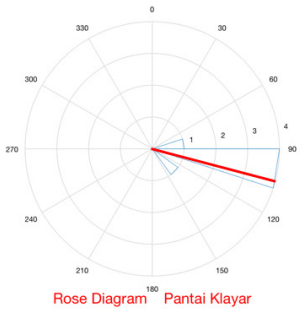

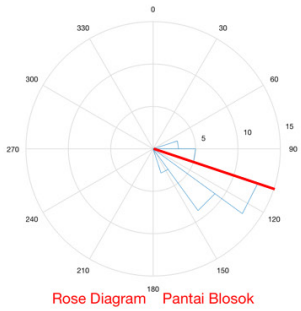

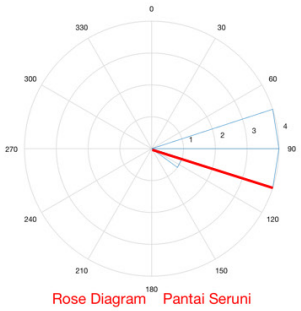

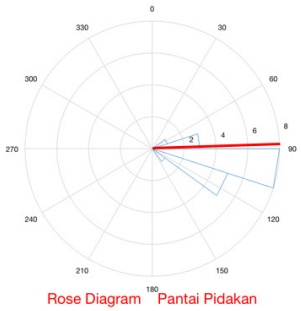

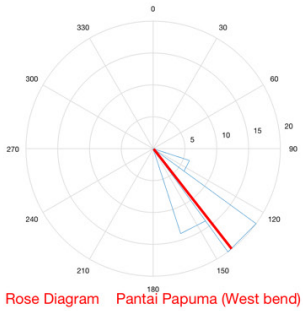

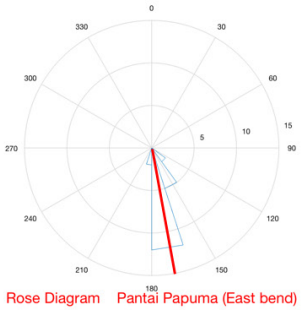

Mean orientations (azimuth) and dip directions of imbricate coastal boulders			
Pantai Nampu	82.53 S	Pantai Pidakan	100.18 S
Pantai Blosok	120.08 S	Pantai Papuma (West)	137.18 W
Pantai Klayar	99.46 S	Pantai Papuma (East)	163.39 E
Pantai Seruni	90.34 S		

Figure 12. Rose diagrams of boulder strike directions for each of the beaches near Pacitan and at Pantai Papuma in East Java. Red line shows the general orientation of the coastline. Pantai Papuma is divided into two diagrams because the beach has a sharp bend; thus, strikes were taken from both the west and east sides of the bend. Strikes from Pantai Pasir Putih were not taken.

2.4 Dimensional Statistical Analyses

Table 1. The Five Largest Imbricated Boulders at Each Beach.

Five largest imbricated boulders at each beach						
	a axis m	**b axis m**	**c axis m**	**Surface area (Sa) m^2**	**Volume (V) m^3**	**Sa/V m^-1**
Pantai Nampu	3.46	1.18	0.22	4.09	0.9	4.55
	2.04	1.74	0.48	3.55	1.71	2.08
	1.54	1.05	0.2	1.62	0.33	4.91
	1.53	0.95	0.22	1.46	0.33	4.43
	1.49	0.92	0.24	1.38	0.34	4.06
Pantai Klayar	2.19	2.05	0.2	4.49	0.9	4.99
	2.13	1.48	0.19	3.16	0.61	5.19
	1.84	1.42	0.17	2.62	0.45	5.83
	1.16	1.04	0.17	1.21	0.21	5.77
	1.05	0.53	0.16	0.56	0.09	6.23
Pantai Blosok	3.5	2.5	0.34	8.75	2.98	2.94
	3.49	0.98	0.36	3.43	1.24	2.77
	3.47	1.1	0.36	3.82	1.38	2.77
	3.2	1.87	0.23	5.99	1.38	4.35
	2.8	2.4	0.24	6.72	1.62	4.15
Pantai Seruni	2.14	1.26	0.35	2.7	0.95	2.85
	1.82	0.96	0.48	1.75	0.84	2.09
	1.8	1.5	0.15	2.7	0.41	6.59
	1.67	1.55	0.23	2.59	0.6	4.32
	1.6	1.5	0.3	2.4	0.72	3.34
Pantai Pidakan	*4.6	1.2	0.23	5.52	1.27	4.35
	2.76	1.12	0.2	3.1	0.62	5
	1.97	1.5	0.23	2.96	0.69	4.29
	1.85	1.5	0.21	2.78	0.59	4.72
	1.77	1.33	0.19	2.36	0.45	5.25
Pantai Papuma	2.85	2.51	0.4	7.16	2.87	2.5
	2.84	2.7	0.35	7.67	2.69	2.86
	2.43	1.82	0.33	4.43	1.47	3.02
	1.87	1.2	0.24	2.25	0.54	4.17
	1.83	1.2	0.24	2.2	0.53	4.16
Average				3.514	0.99	4.15

***The length of the first boulder listed at Pantai Pidakan is a combination of several closely-aligned boulders that, based on their relation, were likely dislodged and transported during a single wave impaction and were modelled as such**

Large boulders at each beach were measured along three axes to determine their surface area and volumes for use in statistical analyses and wave height modeling. In general, the largest boulders were found to the west of Pacitan at Pantai Blosok. However, in one instance, several large boulders in a row at Pantai Pidakan (Figure 13) were measured together as a single boulder because it was observed that they must have been dislodged, dragged across the intertidal platform >200 m possibly by a single wave as they were still mostly aligned and could be easily pieced together. This grouping constitutes the largest boulder that was measured overall. Most of the boulder fields we discovered were >100 meters in length, with the shortest fields by length at Pantai Nampu and Pantai Klayar, and the longest fields at Pantai Blosok and Pantai Papuma, two beaches that had, on average, the largest boulders as well. Dimensional data of the largest 5 boulders measured for each beach is contained below (Table 1).

Many of the boulder ridges are partially or completely buried by sand along strike from the exposed ridges. Exceptions are the more recent imbricated boulder deposits from the 1994 tsunami. These observations demonstrate the marked difference between storm wave energy, which wash inland with enough energy to carry sand and sometimes pebbles and cobbles over the boulders, but not additional boulders. The pebble to cobble size materials are rounded and commonly fill in the interstitial space between the much larger, angular boulders.

Figure 13. (Left) A train of several boulders that were probably excavated simultaneously during a single wave impaction from the carbonate platform a Pantai Pidakan based on their alignment. (Right) Boulder grouping measured at Pantai Pidakan.

A histogram, containing the volumes of all the imbricated boulders measured at each coastal boulder field, was developed for each beach location (Figures 14-19). Besides measuring the five largest boulders, boulders were randomly chosen at each location in an attempt to obtain a representative mean size of the boulder field. The fields with the greatest number of boulders were Pantai Blosok and Pantai Papuma, and this is reflected in the data; however, at no field was every boulder measured. All of the boulder accumulations have fairly similar, right-skewed distributions with most of the boulders averaging roughly 0.5 m^3 in volume. Of the largest boulders, none are much greater than 3 m^3. Additionally, statistical analyses of the mean, median, mode boulder volume were also calculated, as well the overall standard deviation, variance, skewness, and kurtosis for each location.

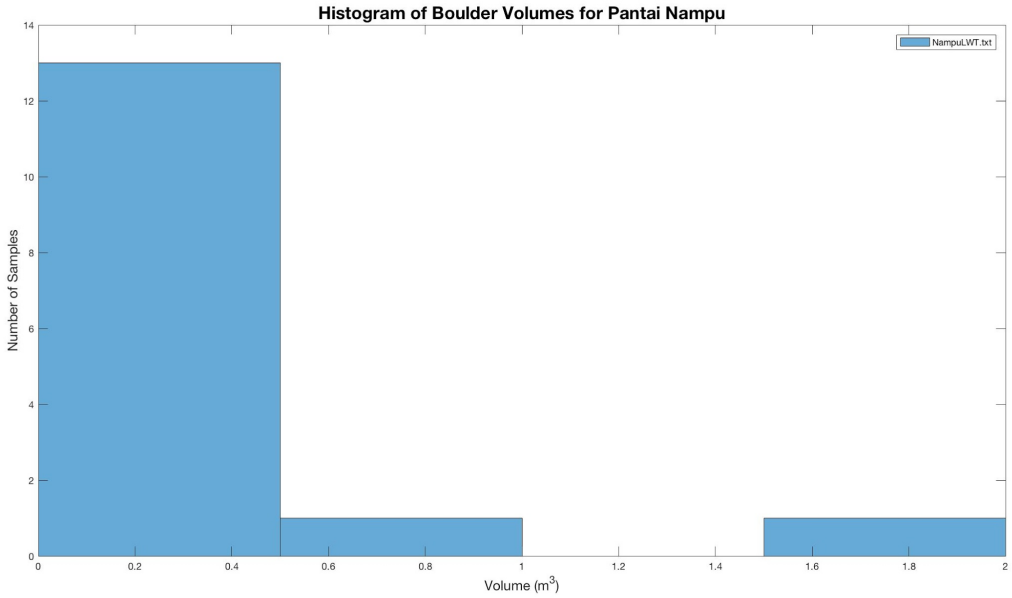

Figure 14. Histogram of all boulder volumes measured at Pantai Nampu. Statistical analyses of the boulders yield: mean = 3.15e-01, median = 1.15e-01, mode = 3.81e-03, standard deviation = 4.54e-01, variance = 2.06e-01, skewness = 2.14e+00, and kurtosis = 6.98e+00.

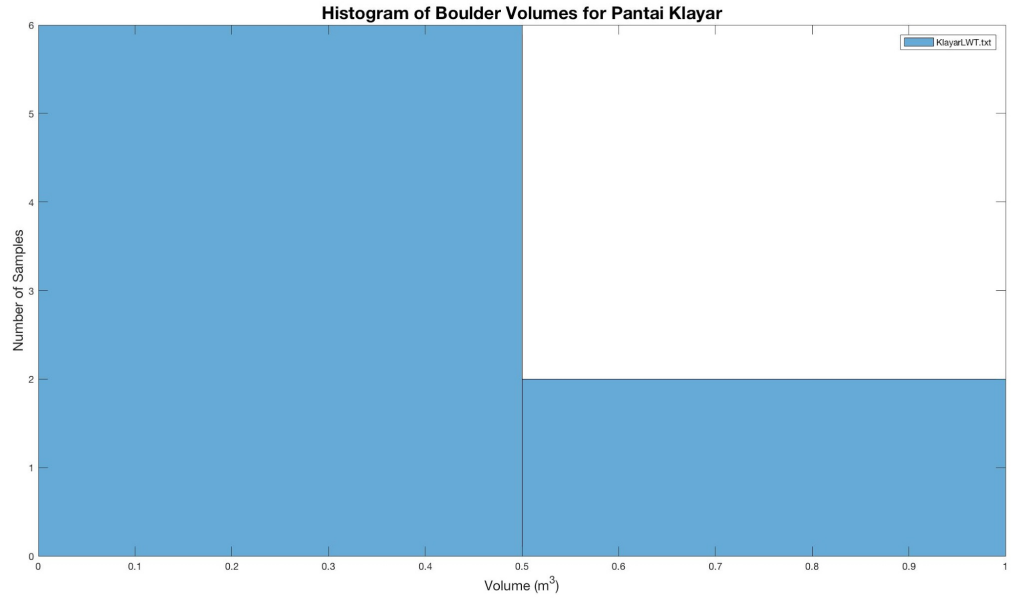

Figure 15. Histogram of all boulder volumes measured at Pantai Klayar. Statistical analyses of the boulders yield: mean = 3.18e-01, median = 1.60e-01, mode = 8.90e-02, standard deviation = 3.02e-01, variance = 9.09e-02, skewness = 9.80e-01, and kurtosis = 2.55e+.

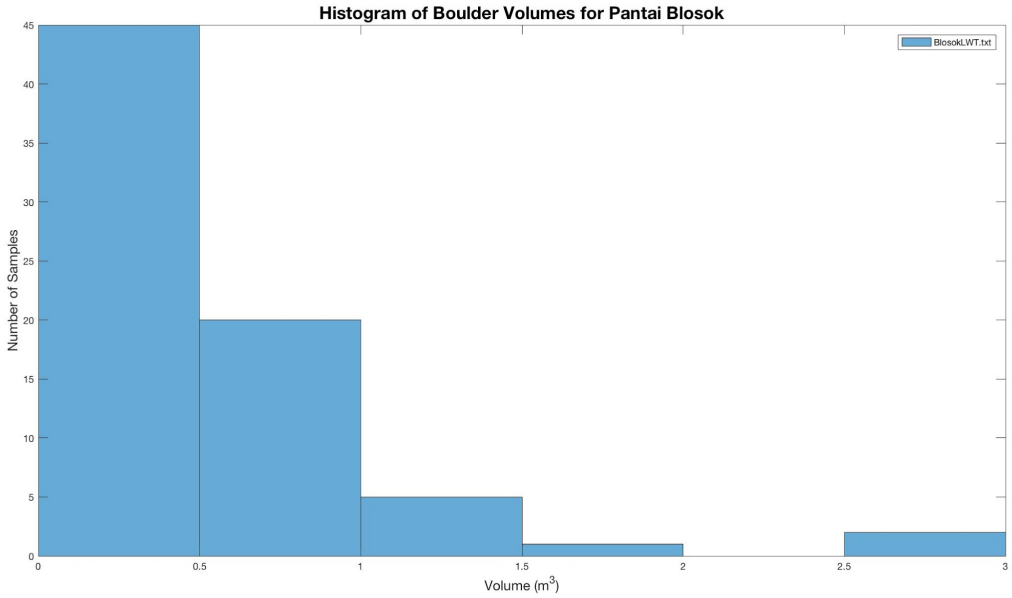

Figure 16. Histogram of all boulder volumes measured at Pantai Blosok. Statistical analyses of the boulders yield: mean = 5.20e-01, median = 3.92e-01, mode = 6.57e-02, standard deviation = 5.38e-01, variance = 2.90e-01, skewness = 2.71e+00, and kurtosis = 1.21e+01.

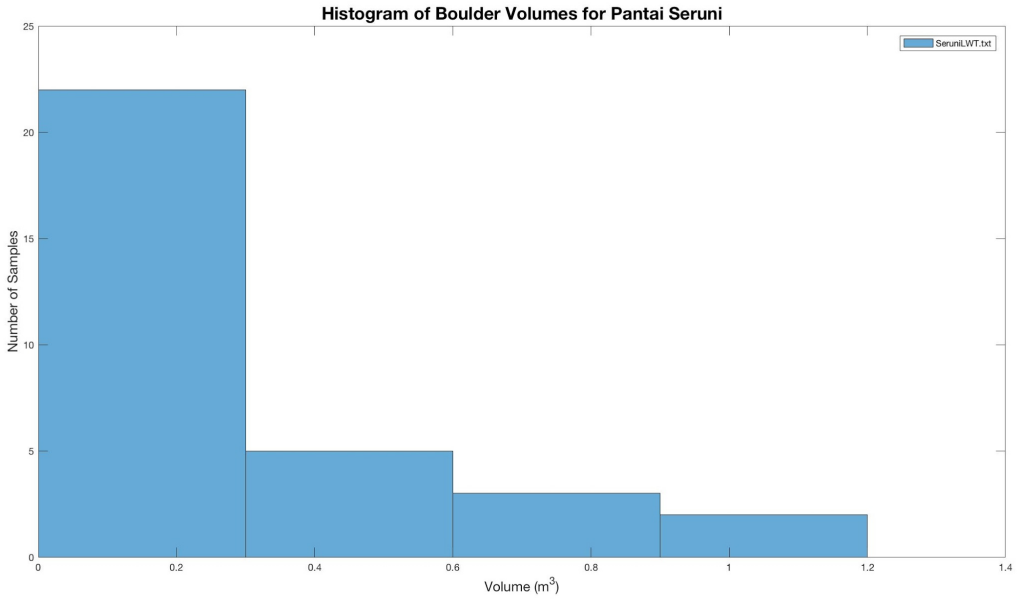

Figure 17. Histogram of all boulder volumes measured at Pantai Seruni. Statistical analyses of the boulders yield: mean = 2.94e-01, median = 1.60e-01, mode = 4.62e-03, standard deviation = 2.96e-01, variance = 8.78e-02, skewness = 1.29e+00, and kurtosis = 3.59e+00.

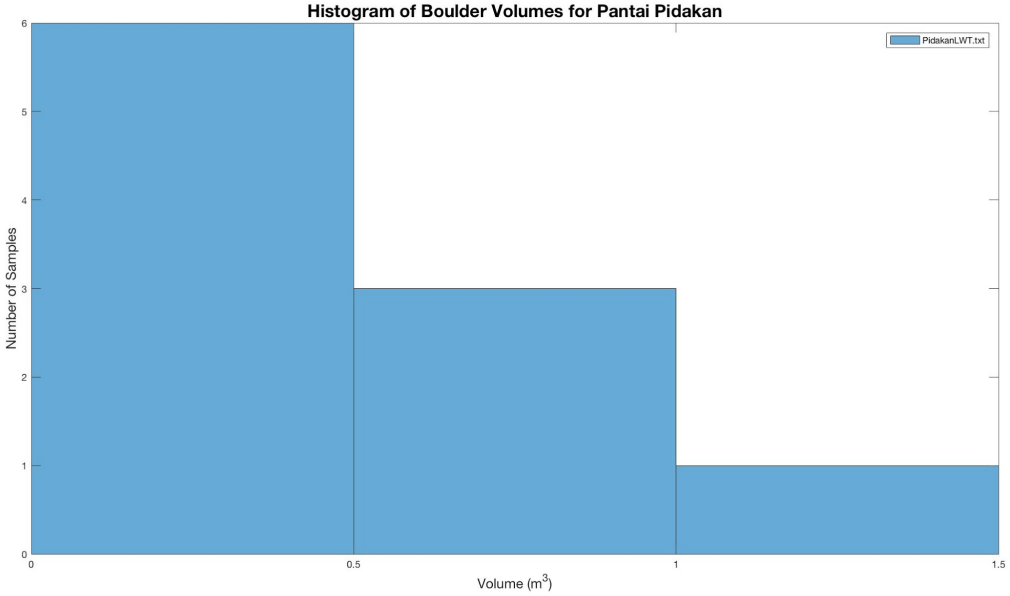

Figure 18. Histogram of all boulder volumes measured at Pantai Pidakan. Statistical analyses of the boulders yield: mean = 4.78e-01, median = 4.71e-01, mode = 1.39e-01, standard deviation = 3.46e-01, variance = 1.20e-01, skewness = 1.11e+00, and kurtosis = 3.72e+00.

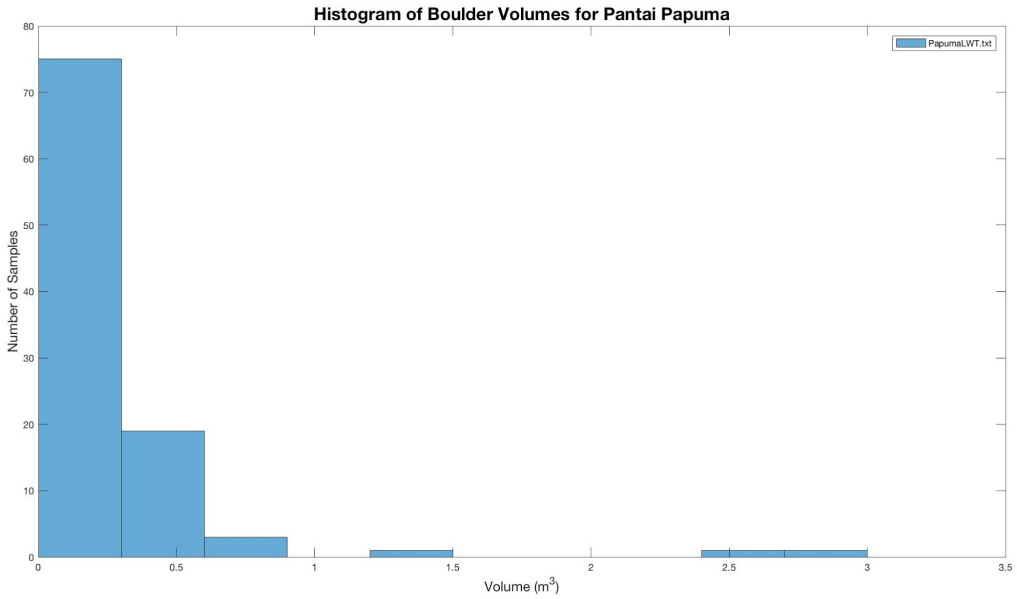

Figure 19. Histogram of all boulder volumes measured at Pantai Papuma. Statistical analyses of the boulders yield: mean = 2.68e-01, median = 1.73e-01, mode = 3.11e-01, standard deviation = 4.06e-01, variance = 1.65e-01, skewness = 5.03e+00, and kurtosis = 3.04e+01.

2.5 Hydrodynamic Wave Height Modeling

Tsunami waves and waves caused by large tropical storms are known to dislodge boulders from joint bound platforms and carry them inland but require different wave heights to do so because of differences in how fast they travel. Tsunami wave trains move at much higher velocities, approximately 28–83 m/s across the continental shelf and 10 m/s at shore, than storm waves, whose periods are much shorter (Bryant 2001). Because of this disparity, a tsunami wave is able to provide the overtopping force necessary to dislodge and transport a boulder inland from the intertidal platform with a much smaller wave than a storm wave can.

Nott (2003) developed hydrodynamic equations for approximating the lift and transport of a boulder for boulders that are sitting submerged on the ocean floor, exposed subaerially, and for boulders locked in a joint bounded block along the intertidal platform near the "toe" of the beach. In Nott's joint bounded block scenario, it is assumed that the boulders must be overtopped by a tsunami or storm wave high enough and fast enough to pluck slabs of rock from the intertidal platform and drag them on shore to form a coastal boulder field or ridge.

The joint-bounded block scenario typically produces wave height estimations with the largest values because it assumes that the boulders were in situ to begin with. We use the joint-bounded block scenario to model the boulder fields that were discovered because they fit this description best. All of the fields near Pacitan, with the exception of Pantai Nampu and possibly Pantai Seruni, exhibit clear evidence of beach rock boulders being lifted from the carbonate platform in the form of excavations that are similar to what Nott describes. Additionally, in hazard assessment, modelled values from this scenario may be seen as the most useful because they are less likely to underestimate the lower wave height limit of past events.

In such a scenario, boulder transport is initiated when the lift force moment equals or

exceeds restraining force moment. Nott (2003) defines the lift force moment as:

lift force moment = (0.5 * density of water at 1.02 g/ml * Nott's coefficient of lift at 0.178 * b axis of the boulder * c axis of the boulder * flow velocity^2) * b axis of the boulder / 2

He defines the restraining force moment as:

restraining force moment = (density of the beachrock boulder at 2.4 g/cm^3 - density of water at 1.02 g/ml) * (a axis of the boulder * b axis of the boulder * c axis of the boulder) * gravitational constant at 9.8 m/s * b axis of the boulder / 2

Simplifying these equations and assuming similar wave type parameters in terms of flow velocity for a tsunami versus a storm, where a tsunami is roughly four times faster, allows us to model these two scenarios separately using the following:

1) Minimum height of storm wave needed to dislodge, transport, and deposit boulders = (((density of beachrock boulder - density of water) / density of water) * a axis of the boulder) / (coefficient of lift)

2) Minimum height of tsunami wave needed to dislodge, transport, and deposit boulders = (0.25 * ((density of beachrock boulder - density of water) / density of water) * a axis of the boulder) / (coefficient of lift)

Histograms (Figures 20-25) comparing the minimum heights of a storm wave and tsunami needed for boulder dislodgement at each beach were produced using Nott's (2003) equations. As shown by differences in their relative bin sizes, blue storm wave height uncertainties are greater than red tsunami height uncertainties for each beach because they exhibit greater disparity between their highest and lowest minimum wave height values.

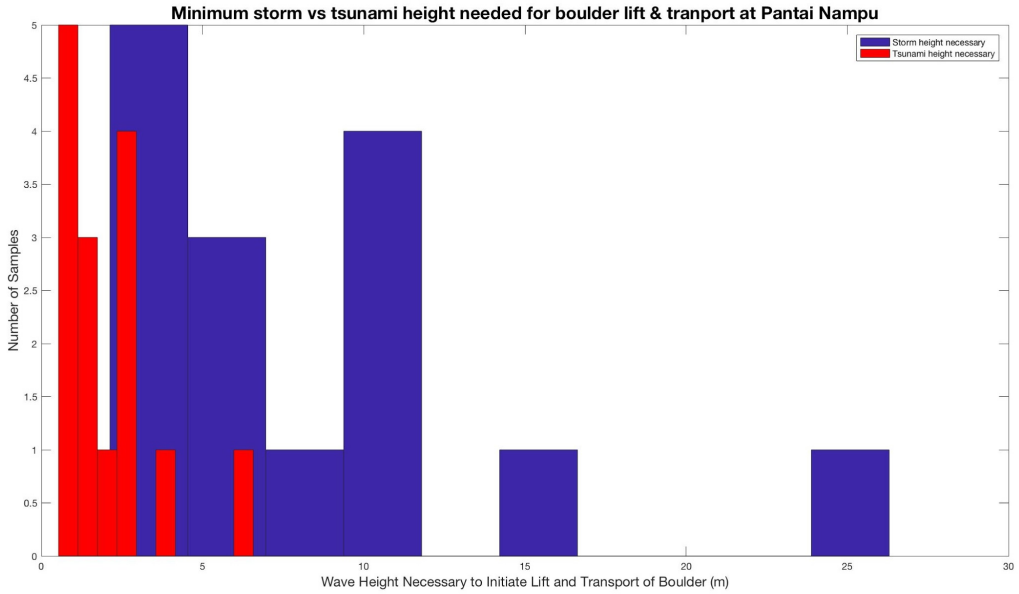

Figure 20. Histogram of all the minimum storm and tsunami wave heights needed for dislodgement, transport, and deposition of beachrock boulders measured at Pantai Nampu based on hydrodynamic equations from Nott's (2003) joint-bounded boulder scenario.

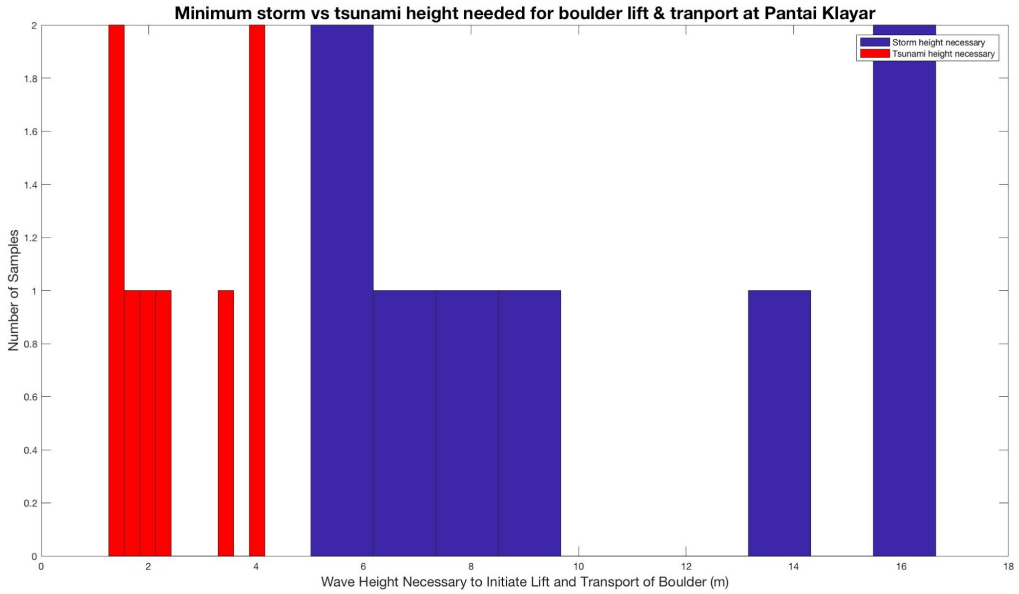

Figure 21. Histogram of all the minimum storm and tsunami wave heights needed for dislodgement, transport, and deposition of beachrock boulders measured at Pantai Klayar based on hydrodynamic equations from Nott's (2003) joint-bounded boulder scenario.

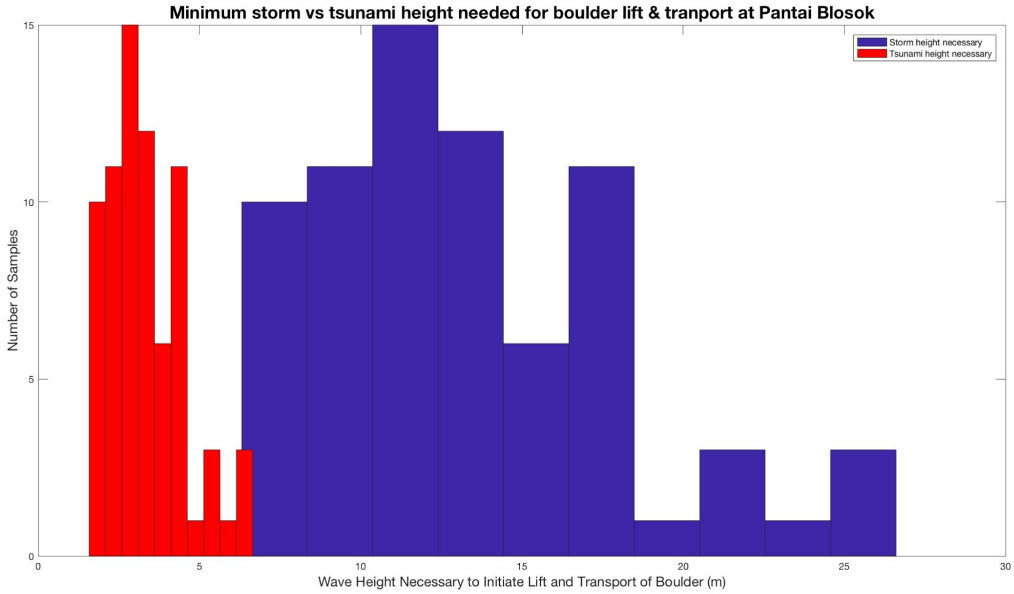

Figure 22. Histogram of all the minimum storm and tsunami wave heights needed for dislodgement, transport, and deposition of beachrock boulders measured at Pantai Blosok based on hydrodynamic equations from Nott's (2003) joint-bounded boulder scenario.

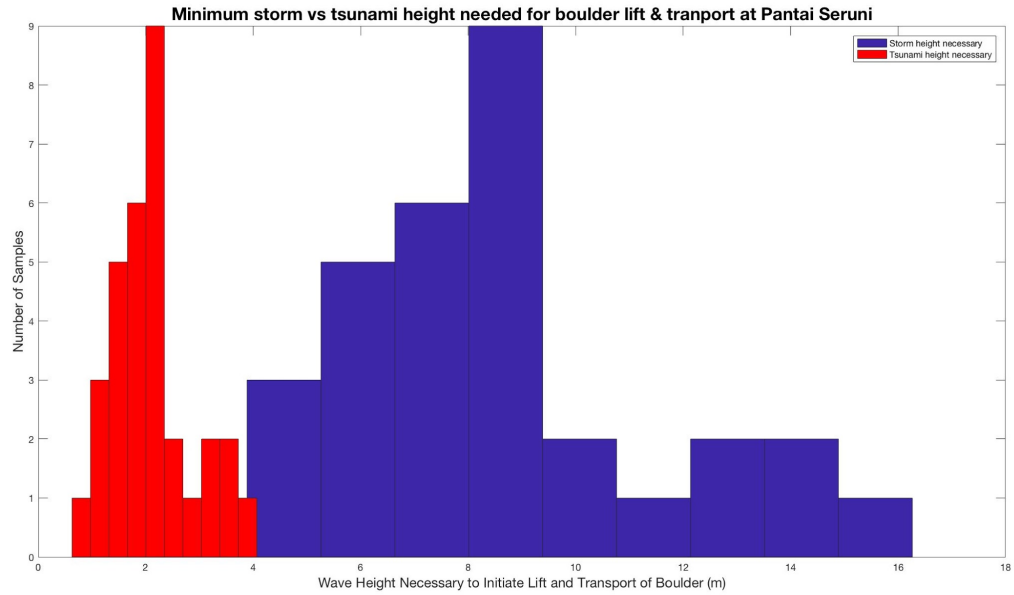

Figure 23. Histogram of all the minimum storm and tsunami wave heights needed for dislodgement, transport, and deposition of beachrock boulders measured at Pantai Seruni based on hydrodynamic equations from Nott's (2003) joint-bounded boulder scenario.

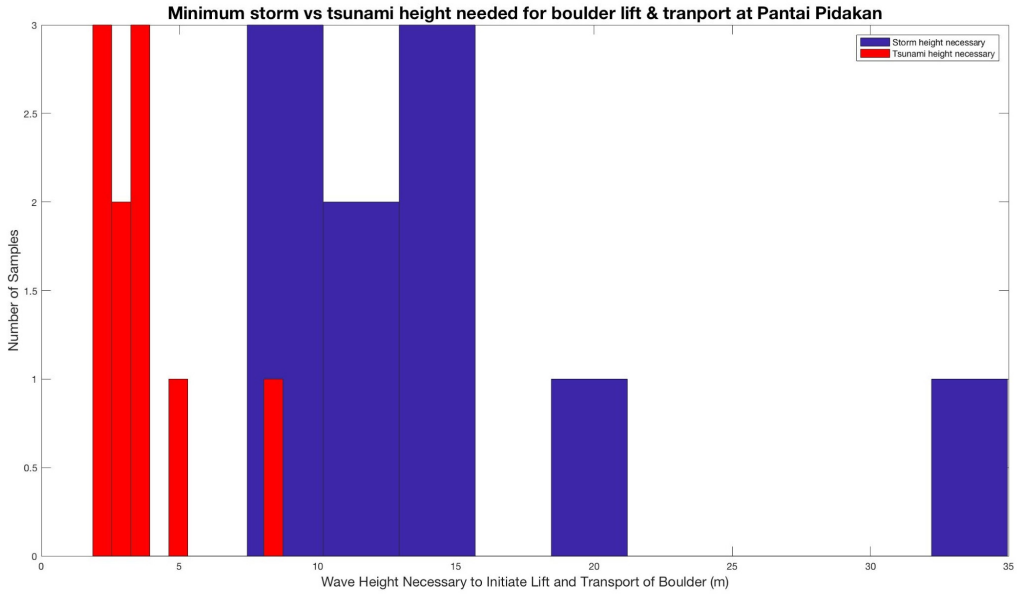

Figure 24. Histogram of all the minimum storm and tsunami wave heights needed for dislodgement, transport, and deposition of beachrock boulders measured at Pantai Pidakan based on hydrodynamic equations from Nott's (2003) joint-bounded boulder scenario.

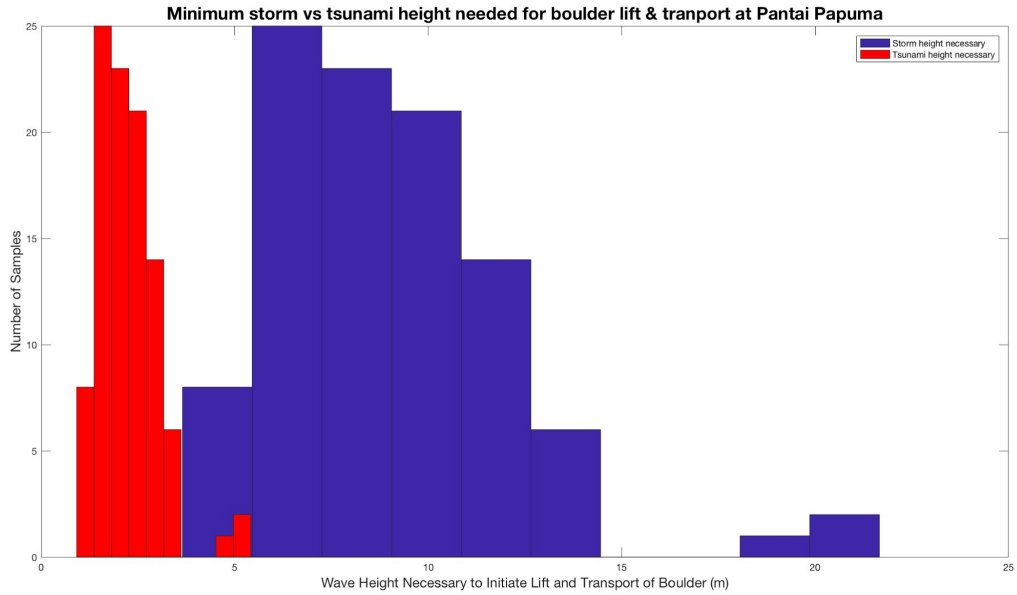

Figure 25. Histogram of all the minimum storm and tsunami wave heights needed for dislodgement, transport, and deposition of beachrock boulders measured at Pantai Papuma based on hydrodynamic equations from Nott's (2003) joint-bounded boulder scenario.

2.6 High Tide Experiment

A simple experiment was conducted at Pantai Seruni during an annual high tide event forecast by Badan Meteorologi Klimatologi dan Geofisika (BMKG) Pacitan to produce a swell with waves as tall as 5 meters. To initiate the experiment, several large boulders were marked and pushed off a nearby coastal cliff onto the wave cut platform just below and offshore in front of the imbricate boulder field the evening before the high tide was to occur. The initial positions were recorded by high resolution drone surveys conducted by Michael Bunds (UVU). Returning the day after the event, we observed that the largest boulders had disappeared entirely from the carbonate platform, but four of the smaller boulders had been re-imbricated onto the boulder field, which was elevated approximately 1-2 meters above mean tide. We observed no new, unmarked boulders on the platform, and the largest, previously-marked boulder that was re-imbricated measured 110 cm * 44 cm * 16 cm (Figure 26). When dimensions for the largest boulder are used with Nott's (2003) submerged boulder scenario, the equation produces a minimum storm height lift and transport value of 1.49 m, which is less than the expected high tide but not by much, considering the site of the boulder accumulations was already elevated relative to mean tide.

Figure 26. (Left) Coastal boulder accumulations at Pantai Seruni. (Right) The largest re-imbricated boulder from our high tide experiment.

Nott's equation for lift and transport of a submerged boulder simply lying on the ocean floor is described as follows:

> Minimum height of storm wave = ((density of beachrock at 2.4 g/m^3 - density of seawater at 1.02 g/ml) / density of seawater) * 2 * a axis) / (Nott's coefficient of drag at 2 * (a axis * c axis * b axis^2) + Nott's coefficient of friction at 0.178)

It should additionally be noted, however, that both Pantai Seruni and Pantai Nampu have prominent coastal cliff walls immediately adjacent to the boulder fields that were observed to produce substantial wave reflections and amplifications, something that was not observed at any other of the coastal boulder fields and that may affect the minimum storm and tsunami wave height values we calculated.

2.7 Radiocarbon Analyses

We sampled three different locations for radiocarbon dating: three imbricated coral boulders at Pantai Blosok, one imbricated coral boulder at Pantai Pidakan (Figure 27), and a large shell emplaced in an imbricated boulder at Pantai Seruni. The radiocarbon chronology results (Figure 28) indicate a variety of ages for the three beaches, with the youngest coral boulders in Pantai Blosok calibrated to around 1861 AD +/-22 (Table 2). If the boulder was imbricated during a tsunami, then this date may possibly correlate with either the 1840 or 1859 known tsunamigenic events that hit Pacitan or a number of other seismic events that occurred around the mid to late 19th century in that region as recorded in the Wichman catalogue.

Figure 27. Coral boulder at Pantai Pidakan.

The wide spectrum of ages for the imbricate coral boulders at Pantai Blosok and among the three beaches as a group may be a result of many factors but is not unusual for coastal boulder accumulations. Calibrating multiple coral ages for one coastal boulder field, or among set of closely distributed boulder fields, may indicate that the field has amassed over a series of events (Nott 1997, 2004); however, a greater number of samples is needed to determine whether these calibrated ages significantly correlate with any tsunamigenic earthquake event. Additionally, age uncertainties may be much greater than radiocarbon chronology results indicate because coral boulders experience varying degrees of erosion along the coast over time and can be reworked by tsunamigenic events occurring after their initial deposition.

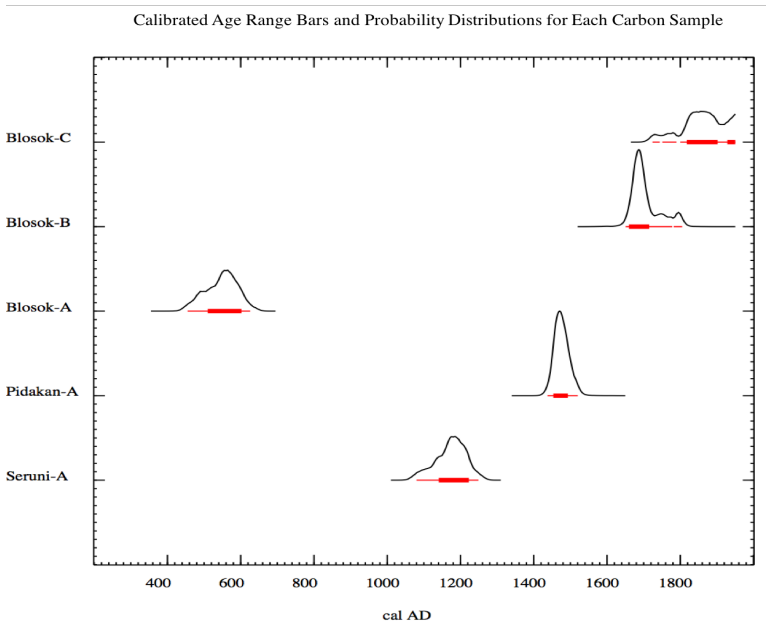

Figure 28. CALIB Calibrated radiocarbon analyses of boulders and a shell from three coastal boulder fields: Pantai Blosok, Pantai Pidakan, and Pantai Seruni.

Table 2. Table 2. Radiocarbon Chronology of a Shell and Coral Boulders Found Wedged Within Five Imbricated Boulder Fields Near Pacitan, Indonesia.

Radiocarbon chronology of a shell and coral boulders found wedged within five imbricated boulder fields near Pacitan, Indonesia			
Location	**Description**	**d13C Corrected Age**	**d13C Calibrated Ages (95.4 - 2 sigma)**
Pantai Blosok-C	Imbricated coral boulder	555 +/- 22 YBP	1861 AD
Pantai Blosok-B	Imbricated coral boulder	677 +/- 23 YBP	1692 AD
Pantai Blosok-A	Imbricated coral boulder	1930 +/- 23 YBP	551 AD
Pantai Pidakan-A	Imbricated coral boulder	913 +/- 22 YBP	1474 AD
Pantai Seruni-A	Shell on boulder	1307 +/- 23 YBP	1177 AD
Weighted mean deltaR: 72			
Standard deviation (square root of deviance): 9			
Radiocarbon dates calibrated using CALIB program, shell and corals corrected for marine reservoir			
Radiocarbon analysis report from The University of Georgia Center for Applied Isotope Studies			

3. ComMIT Tsunami Modelling and Inundation Maps

3.1 Approximating a Past Rupture Magnitude for Boulder Accumulations Near Pacitan

We developed tsunami models of various earthquake magnitudes near Pacitan to approximate the minimum size of an earthquake necessary that could produce the max boulder tsunami wave heights we calculated using Nott's joint bounded block equation. In order to perform this modelling, two major assumptions were made: 1) that all of the largest boulders were deposited sometime during the same event, and 2) that the rupture area for the event occurred along a portion of the seismic gap just south of Pacitan, as indicated in the bottom right corner of Figure 9. After steadily increasing the offshore magnitude of the earthquake over many modelling runs, the final result that best fit our previous MatLAB wave height modelling data had a moment magnitude of 8.4 and produced a tsunami with a maximum wave amplitude of 16.59 m, a minimum wave amplitude of -8.37 m, a maximum flow depth of 13.27 m, and a maximum current speed of 13.22 m/s. It may, therefore, be assumed that if all of the boulder fields west and east of Pacitan were deposited during a single event, then, according to both Nott's joint bounded block equations and our tsunami modelling, the minimum magnitude of an earthquake needed to emplace these boulders would be at least 8.4 Mw, but possibly higher. While this scenario seems unlikely, considering the many historical earthquakes and tsunamis recorded near Pacitan over the last 430 years, it is not outside the realm of possibility, considering that Pacitan has had earthquakes whose duration was as long as 2 minutes. Typically, earthquakes with magnitudes in the high sevens produce minute-long shaking, those with magnitude eights produce two-minute long shaking, and those with high eights produce three-minute shaking.

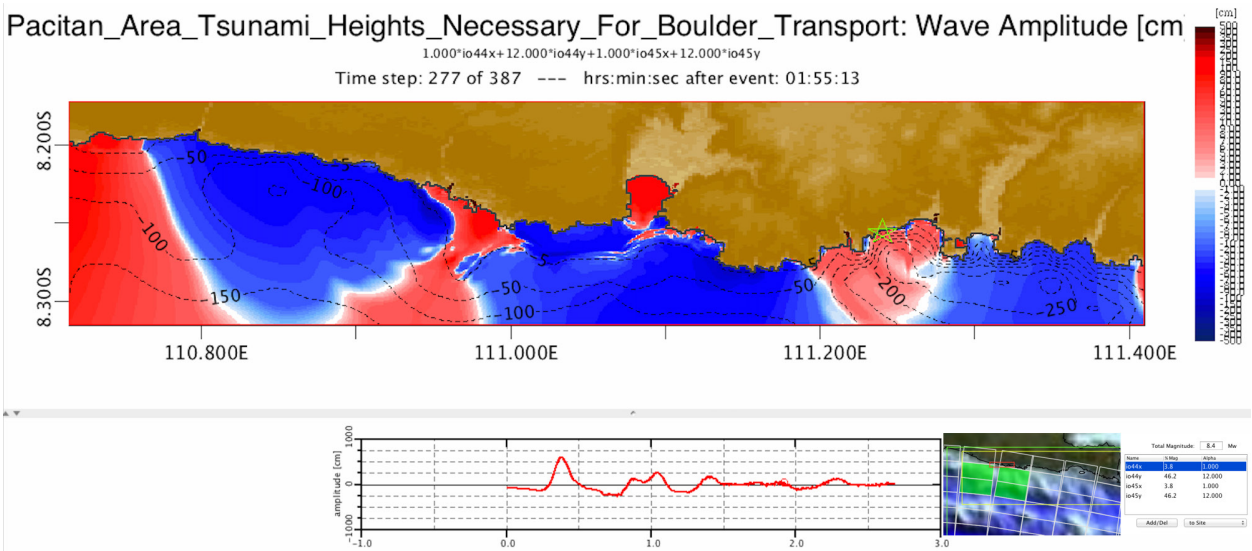

Figure 29. ComMIT tsunami modelling of an 8.4 Mw earthquake just offshore Java. The grid in the bottom right corner shows the rupture area locations and slip magnitudes that were assumed. The green star is the position of the time series data.

In order to perform our tsunami modelling, we used ComMIT (Titov et al. 2011). ComMIT is an interface developed for NCTR (NOAA's Center of Tsunami Research) that utilizes their "Method Of Splitting Tsunamis" (MOST). MOST uses shallow water equations and prerecorded or custom made fault plane solutions to model Earthquake originated tsunamis. The process is broken up into three steps/grids with each grid (A, B, and C) containing progressively higher resolution bathymetry and topography. These three steps include: earthquake, transoceanic propagation, and inundation of dry land. Bathymetry is from ETOPO1 1 arc-minute gridded global relief model produced by the NOAA National Geophysical Data Center and has been interpolated from 60 arc seconds to 3 arc seconds. Topography is from the CGIAR SRTM 90m version 4 digital elevation model produced by the CGIAR Consortium for Spatial Information.

3.2 Tsunami Modelling and Inundation Maps Assuming Total Rupture of Offshore Java's Current Seismic Gap

In addition to approximating past events, we also model a potential worst-case scenario for Pacitan based on our previous estimations of the current offshore hazard, which has the potential of producing an earthquake with a >9.0 Mw. To perform this modelling, we assume a slip distribution along the subduction interface similar to Japan's 2011 earthquake and tsunami. The slip from NOAA's 2011 Japan tsunami model (Titov et al. 2016) of 27.39 m was used for the epicenter. We have portrayed our results in an inundation map of Pacitan (Figure 30).

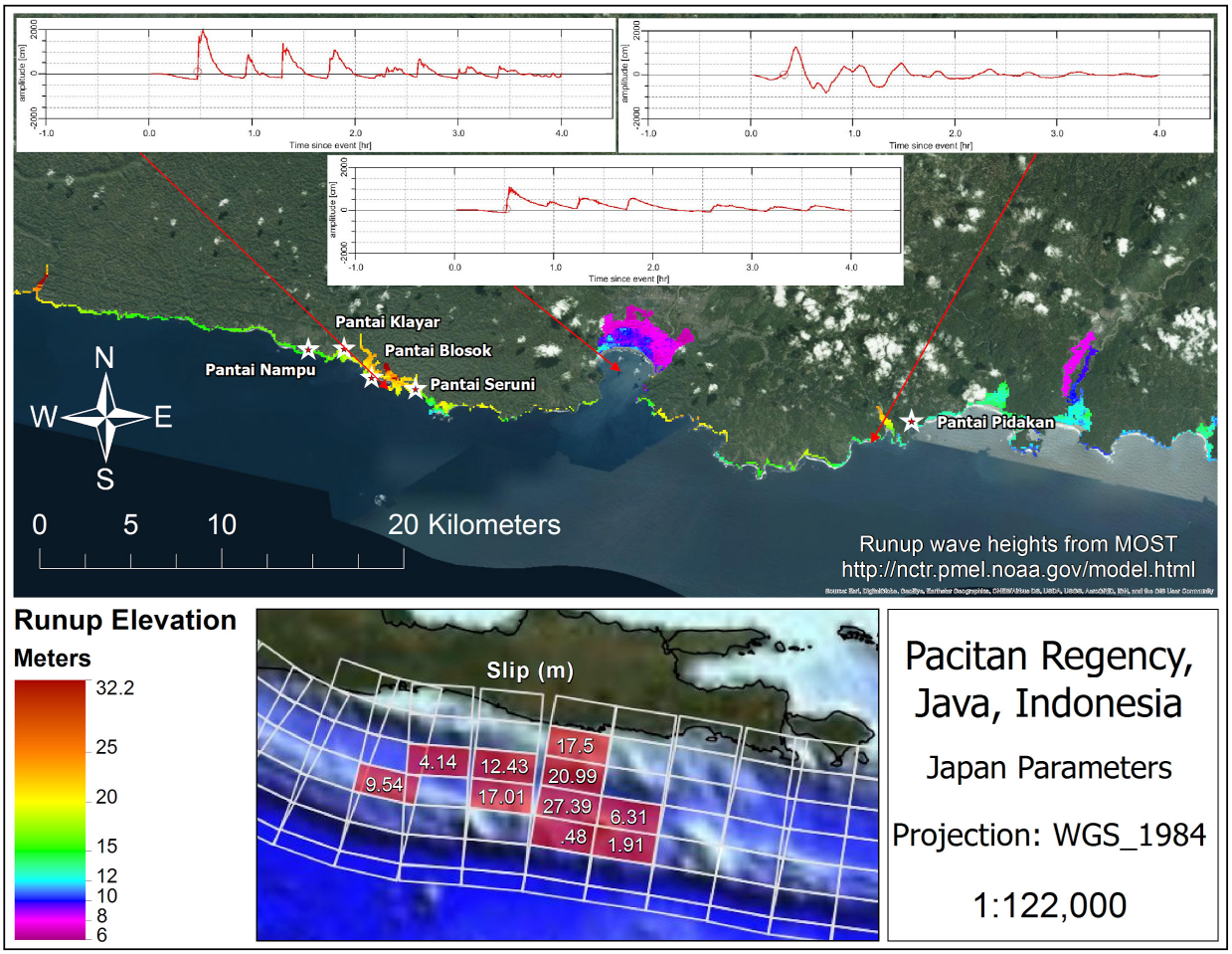

Figure 30. Inundation map of Pacitan and five nearby beach locations with coastal boulder accumulations. The slip distribution along the fault is similar to Titov et al.'s (2016) 2011 Japan earthquake and tsunami model. Wave amplitudes at three locations indicated by red arrows are shown in cm. Rupture areas and magnitudes are shown in the bottom grid. Runup elevations and inundation along the coast are shown.

Pantai Blosok is seen to have the highest runups, while Pacitan has relatively small runups but is deeply inundated. The coastal populations at these five locations are much smaller relative to those at East Java but are still endangered by tsunami hazards.

We also model a potential worst-case scenario for the entire offshore seismic gap along the eastern portion of the Sunda trench and include an inundation map of the most populated portion of East Java. Based on our previous estimations of the current offshore hazard for East Java and Bali, parameters for slip along the fault were also chosen with a >9.0 Mw scenario in mind. Because of the thousands of models and hours that would be needed to try and include all possible tsunami scenarios, we opted for creating an epicenter independent model with the same epicenter parameters spanning the whole fault from East to West. Because open ocean waves are mostly linear and islands were analyzed perpendicular to the tsunami, differences from this scenario and one with the epicenter perpendicular to any coastal area were observed in other models to have similar inundation values. The slip from NOAA's 2011 Japan tsunami model (Titov et al. 2016) of 27.39 m was used for the epicenter in all models (50 km long North to South) with similar 50 km fault plane solutions to the North and south of the epicenter area generating 21 m of slip (about the same slip from the next highest fault plane solution from Japan.)

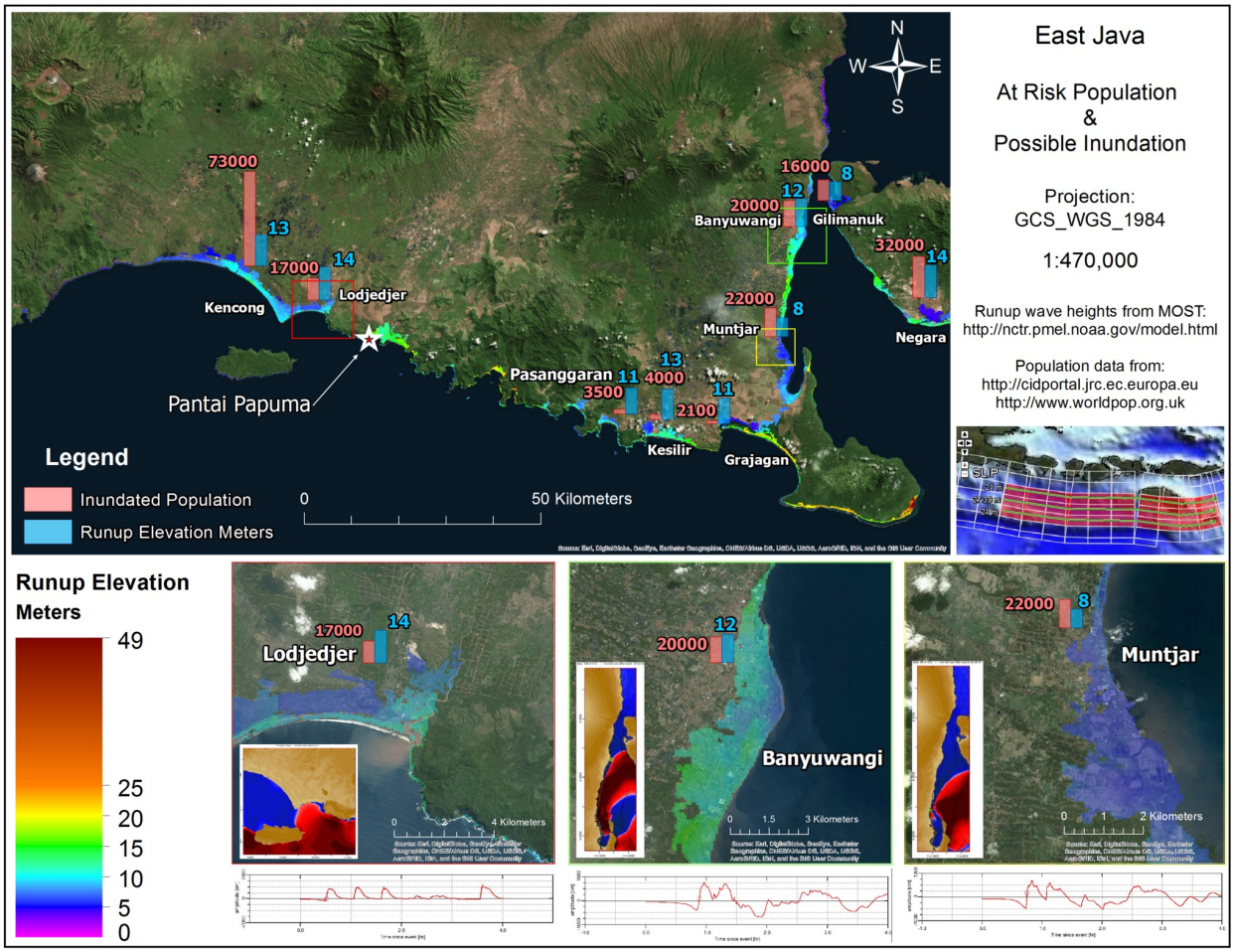

Figure 31. Inundation map of East Java assuming slip parameters similar to Titov et al.'s (2016) 2011 Japan earthquake and tsunami model. Time series showing wave amplitudes at three locations, Lodjedjer, Banyuwangi, and Muntjar are also shown in cm. Rupture areas and slip parameters are shown in the grid on the right. Runup elevation and inundation, as well as inundated populations along the coast are shown. Pantai Papuma is also shown. Approximately 307,000-501,000 people in East Java may be directly affected by an event of this magnitude.

Inundation maps for both Pacitan and East Java (Figure 31) were created with data from ComMIT exported into ArcMap from Esri. Population within the inundation zone for East Java was calculated using two data sources: "World Pop" projected 2020 census distribution (www.worldpop.org.uk) and the 2015 "European Commission, Joint Research Centre" (JRC) census distribution (data.europa.eu). Both data sets are distributed on the basis of regional population surveys and satellite imagery. Through ArcMap GIS tools, data was clipped from inundated areas, and the sums were analyzed from both sources. Because resulting data varied

from both sources, and because of human decision and error, the projected population at risk may be viewed as a rough estimate.

3.3 Tsunami modelling limitations

Tsunami forecasting and modelling is an inherently biased procedure because it uses rough estimates of the size, magnitude, and location of seismic events as inputs, and it is important to recognize its limitations. The ComMIT manual explicitly states that because most of the bathymetry downloaded from the NOAA server is low-resolution and has received limited manual review, it should not be used for hazard mapping. The figures made from ComMIT should be analyzed with this disclaimer in mind and are only an estimated projection of possible tsunami data. However, because of the millions of lives at risk and a lack of better current bathymetry data available, using these data can still be helpful for mitigation efforts and demonstration purposes.

Both bathymetry and the use of the epicenter independent modeling introduce an uncertainty that must be accounted for. It is possible despite using liberal parameters, that inundation could be higher than projected because of actual bathymetry, slope failures, or other different earthquake scenarios. Variability in land surface friction along topography is also impossible to account for. Because of these limitations and others, it is important that the data displayed in these figures not be viewed as an absolute or sole reference for mitigation efforts. Tsunami modeling along the Sunda trench would be substantially improved by the obtainment of high-resolution bathymetry.

4. Discussion

4.1 Comparing Coastal Boulder Accumulations Near Pacitan with Those at Pantai Papuma

Because the imbricate coastal boulder field at Pantai Papuma was deposited during a recent tsunami event, and owing to its nearby and similar coastal setting with the other coastal boulder fields near Pacitan, Pantai Papuma may be used as a standard of comparison with the other beaches under the assumption that they were all tsunami emplaced. Pantai Papuma was deposited by a tsunami wave train (Fig. 32) that resulted from a 7.9 Mw earthquake along the offshore trench adjacent East Java. During the event, the southeast Java coastline experienced various runup heights ranging from 1-14 m (Synolakis et al. 1995). Tsuji et al. (1995) performed a field survey of the southern coast of Jember regency at a location near Pantai Papuma within three weeks of the event and observed that the maximum runup height near that area varied between 4-10 m. According Nott's (2003) joint-bounded boulder scenario, the largest boulder we recorded for that area required a tsunami with a minimum wave height of approximately 5 m to dislodge, transport, and emplace it on the beach. This discrepancy in wave observed versus model tsunami wave heights near and at Pantai Papuma is not unusual because tsunami wave speed may vary significantly along the coast.

Figure 32. (Left) More than five layers of boulders stacked on each other at Pantai Papuma, possibly where two large tsunami waves collided. (Right) Several large, imbricated boulders at Pantai Papuma. Orange measuring tape for scale.

Three of the fields near Pacitan have larger boulders than any that are found at Pantai Papuma. These were Pantai Nampu, Pantai Blosok, and Pantai Pidakan, whose largest boulders require a tsunami with wave heights of roughly 6, 7, and 8 m respectively. Of these three beaches, Pantai Blosok and Pantai Pidakan are the most similar in terms of topography with Pantai Papuma because each has no cliff wall directly adjacent the imbricated boulder deposit. Pantai Blosok, Pantai Pidakan, and Pantai Papuma also similarly have long, flat carbonate platforms that extend several hundred meters away from the toe of the beach. The carbonate platforms at these beaches can be easily traversed during low tide because the waves at these locations typically break hundreds of meters offshore from the beach. Additionally, each of these three similar beaches exhibit clear excavations, or dislodgements, of boulders that are visible across the carbonate platform directly in front of each of these beaches' boulder deposits. However, Pantai Pidakan had very few boulders relative to either Pantai Blosok or Pantai Papuma and some of its largest boulders were not imbricated onto other boulders as they were at

the other two beaches; instead, the largest boulders at Pantai Pidakan formed a slightly broken line of large blocks across the shore .

It seems plausible, therefore, that if all of the large boulders for each beach were dislodged and emplaced by a tsunami wave train, then the waves that hit beaches both west and east of Pacitan, like Pantai Nampu, Pantai Blosok, and Pantai Pidakan, must have been as large or larger than the waves that hit Pantai Papuma during the 1994 7.9 Mw event, assuming a similar topography, similar coefficient of friction, and similar density of the beachrock.

4.2 Why Are There No Boulders in Pacitan?

There are no wave-emplaced boulder accumulations along the beach directly in front of Pacitan. This may be because Pacitan's coastline forms a large bay and is currently an active depositional setting, which may make it difficult for carbonate beachrock to form just offshore, and none is observed. Pacitan is flanked by rivers on both sides of the city that empty into the bay and regularly deposit sediment; thus, the depositional environment is very different than some of the other coastal beach locations that contain imbricated boulder fields. Moreover, tsunami modelling of a Pacitan's bay area indicates that, while Pacitan is likely to be heavily inundated by a tsunami wave train, it does not experience wave speeds or inland runup heights as great as those near the coastal boulder fields we observed to its west and east. However, the concave, coastal topography that Pacitan's bay exhibits may have a dual effect of amplifying inundation while slowing tsunami wave speed.

4.3 Nott's (2004) Australian Boulders

Tsunami modelling shows tendrils of high wave magnitudes reaching places where Nott (2004) also describes boulder ridge deposits in Northwest Australia near Exmouth Gulf (Figure

33) that are similar to those we discovered along the Java coast. The largest boulder he measured at this area was 2.1 m long and required a minimum tsunami wave height of 4.6 m according to his joint-bounded boulder scenario. He records three oysters and shells at the back of the ridge with radiocarbon chronologies dating around the mid to late 19th century, a time period of heavy seismicity near Pacitan according to the Wichmann catalogues. Nott infers that the boulders were deposited by a tsunami that may have derived from an earthquake along the eastern segment of the Sunda trench. He was able to record the positions of the boulders fields on Exmouth coast before and after several major storms and observed that no new boulders were imbricated, nor were any of the boulders he recorded moved. The storms he observed are much larger than any Java will ever experience. It is possible that boulders from the five beach locations described in this paper near Pacitan and the boulders at Exmouth Gulf may have been emplaced by tsunamis created by the same earthquake.

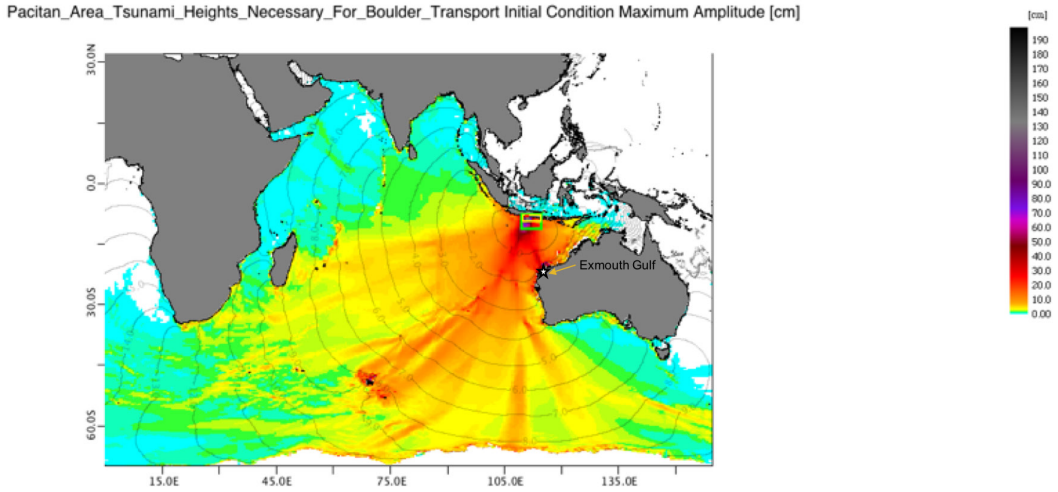

Figure 33. ComMIT global maximum amplitude map showing tendrils of high tsunami wave amplitudes caused by a 8.4 Mw rupture along the trench near Pacitan. Exmouth Gulf in NW Australia where Nott's (2004) boulders were observed receives some of the highest amplitudes.

5. Conclusion

We claim that the imbricate coastal boulder accumulations along beaches west and east of Pacitan were emplaced as a result of tsunami wave impactions derived from one or several

tsunamigenic earthquakes along the trench just offshore from Java. Modern storm waves are rarely, if ever, thought to produce such extensive accumulations of large, imbricated boulders (Young et al. 1996). Moreover, large storms are rarely known to make landfall along Java, and storm wave modelling of these fields indicates that the largest boulders require storm wave heights from 16 to 35 m high, which there is no historical precedent for even in areas along the Australian coast impacted by the largest cyclones ever recorded. A comparison of the fields with a known tsunami deposit at Pantai Papuma also favorably demonstrates that the largest boulders are similar in size and composition to the largest boulders there. Additionally, radiocarbon dating of coral at Pantai Blosok potentially indicates that some of the boulders were emplaced sometime around a period of high seismicity in the region and possibly during one or both of two localized tsunamis that made landfall at Pacitan during the mid-to-late 19th century. Tsunami wave modelling suggests that the boulder fields near Pacitan may have been emplaced as a result of an 8.4 Mw tsunamigenic earthquake along the offshore trench if emplaced all at once. However, a more likely scenario, according to our limited radiocarbon chronology, is that the boulders were emplaced during several separate events over time.

Further surveying for tsunami paleo-markers is needed to better constrain modelling parameters related to the earthquake and tsunami hazards offshore Java and Bali. However, the offshore seismic gap in this region should be seriously considered and, according to current estimates, is potentially capable of producing a >9.0 Mw earthquake. ComMIT tsunami modelling of a megathrust >9.0 Mw quake along the trench near East Java and Pacitan demonstrates that low-lying, coastal elevations, especially those near known imbricate coastal boulder fields, in this region are susceptible to major inundation and 20 m runup heights or more

in some areas. These populations should prepare now by educating the general public about the "20/20/20 principle" (Hall et al. 2017).

References

Ammon CJ, Kanamori H, Lay T, Velasco A (2006) The 17 July 2006 Java tsunami earthquake. Geophys Res Lett 33:L24308. doi:10.1029/2006GL028005

Atwater B (2007) Hunting for Ancient Tsunamis in the Tropics. Eos Transaction AGU, 88(23), Jt. Assem. Suppl., Abstract T24A-01

Badan Meteorologi Klimatologi dan Geofisika (2010) Laporan Gempabumi Mentawai, 25 Oktober 2010, p 18

Bilek SL, Engdahl RE (2007) Rupture characterization and aftershock relocations for the 1994 and 2006 tsunami earthquakes in the Java subduction zone: Geophysical Research Letters, vol 34, L20311, doi: 10.1029/2007GL031357

Brune S, Ladage S, Babeyko AY, Müller C, Kopp H, Sobolev SV (2010b) Submarine landslides at the eastern Sunda margin: observations and tsunami impact assessment. Nat Hazards 54:547–562

Bryant EA (2001) Tsunami—The underrated hazard. Cambridge University Press, United Kingdom

Cidportal: Directory of http://cidportal.jrc.ec.europa.eu/ftp/jrc-opendata/GHSL/GHS_POP_GPW4_GLOBE_R2015A/GHS_POP_GPW42015_GLOBE_R2015A_54009_250/V1-0/, Last access: 23, Aug 2017

Etienne S, Buckley M, Paris R, Nandasena A, Clark K, Strotz L, Chagué-Goff C, Goff J, Richmond B (2011) The use of boulders for characterising past tsunamis: lessons from the 2004 Indian Ocean and 2009 South Pacific tsunamis. Earth-Sci Rev

Felton EA, Crook KAW (2003) Evaluating the impacts of huge waves on rocky shorelines: an essay review of the book 'Tsunami—the underrated hazard'. Mar Geol 197:1–12

Fritz HM, Kongko W, Moore A, McAdoo B, Goff J, Harbitz C, Uslu B, Kalligeris N, Suteja D, Kalsum K, Titov V, Gusman A, Latief H, Santoso E, Sujoko S, Djulkarnaen D, Sunendar H, Synolakis C (2007) Extreme runup from the 17 July 2006 Java tsunami. Geophys Res Lett 34:L12602. doi:10.1029/2007GL029404

Hall S, Pettersson J, Meservy W, Harris R, Augustinawati D, Olson J, McFarlane A (2017) Awareness of tsunami natural warning signs and intended evacuation behaviors in Java, Indonesia. Nat Hazards pp 1-24. doi:10.1007/s11069-017-2975-3

Hamzah L, Puspita NT, Imamura F (2000) Tsunami catalogue and zones in Indonesia. J Nat Disaster Sci 22(1):25–43

Harbitz CB, Lovhølt F, Bungum H (2014b) Submarine landslide tsunamis: how extreme and how likely? Nat Hazards 72:1341–1374. doi:10.1007/s11069-013-0681-3

Harders R, Ranero CR, Weinrebe W, Behrmann JH (2011) Submarine slope failures along the convergent continental margin of the Middle America Trench. Geochem Geophys Geosyst 12:Q05S32. doi:10.1029/2010GC003401

Harris R, Major J (2016) Waves of destruction in the East Indies: the Wichmann catalogue of earthquakes and tsunami in the Indonesian region from 1538 to 1877. In: Cummins PR, Meilano I (eds) Geohazards in Indonesia: earth science for disaster risk reduction. Geological Society, London, Special Publications, pp 441. doi:10.1144/SP441.2

Harris RA, Prasetyadi C (2002) Who's next? Assessing vulnerability to geophysical hazards in densely populated regions of Indonesia. Bridges 2:14–17. doi:10.1144/SP441.2

Kopp H, Flueh ER, Petersen CJ, Weinrebe W, Wittwer A (2006) The Java margin revisited: evidence for subduction erosion off Java. Earth and Planetary Science Letters, vol 242, pp 130-142. doi:org/10.1016/j.epsl.2005.11.036

Lauterjung J, Münch U, and Rudloff A (2010) The challenge of installing a tsunami early warning system in the vicinity of the Sunda Arc, Indonesia. Nat. Hazards Earth Syst. Sci 10:641-646 doi:10.5194/nhess-10-641-2010

Major JR, Harris RA, Robinson JS (2008) Earthquake and tsunami history and hazards of eastern Indonesia. Eos Trans AGU 89(53), Fall Meet. Suppl., Abstract T53E-2009

Maramai A, Tinti S (1997) The 3 June 1994 Java tsunami: a post-event survey of the coastal effects. Nat Hazards 15:31–49

Masson DG, Harbitz CB, Wynn RB, Pedersen G, Løvholt F (2006) Submarine landslides: processes, triggers and hazard prediction. Phil Trans R Soc A 364:2009–2039. doi:10.1098/rsta.2006.1810

Newcomb KR, McCann WR (1987) Seismic history and seismotectonics of the Sunda Arc. J Geophys Res 92(B1):421–439

Nott J (1997) Extremely high-energy wave deposits inside the Great Barrier Reef, Australia: Determining the cause-tsunami or tropical cyclone. Marine Geology. 141, 193–207

Nott J (2003) Waves, coastal boulder deposits and the importance of the pre-transport setting, Earth Planet. Sci. Lett., 210, 269–276

Nott J (2003b) Tsunami or storm waves?—determining the origin of a spectacular field of wave emplaced boulders using numerical storm surge and wave models and hydrodynamic transport equations. Journal of Coastal Research 19, 348 – 356

Nott J (2004) The tsunami hypothesis – comparisons of the field evidence against the effects, on the Western Australian coast, of some of the most powerful storms on Earth, Mar. Geol., 208, 1–12

Paris R, Wassmer P, Lavigne F, Belousov A, Belousova M, Iskandarsyah Y, Benbakkar M, B Ontowirjo, Mazzoni N (2014) Coupling eruption and tsunami records: the Krakatau 1883 case study, Indonesia. Bulletin of Volcano 76 814

Philibosian B, et al. (2017) Earthquake Supercycles on the Mentawai Segment of the Sunda Megathrust in the 17th Century and Earlier, J. Geophys. Res. Solid Earth, 122, doi:10.1002/2016JB013560

Polet J, Thio HK (2003) The 1994 Java tsunami earthquake and its "normal" aftershocks. Geophys. Res. Lett. 30(9), 1474, doi:10.1029/2002GL016806

Post J, Wegscheider S, Mück M, Zosseder K, Kiefl R, Steinmetz T, and Strunz G (2009) Assessment of human immediate response capability related to tsunami threats in Indonesia at a sub-national scale. Natural Hazards and Earth System Sciences 9(4):1075-1086

Rubin CM, Horton BP, Sieh, K, Pilarczyk JE, Daly P, Ismail N, Parnell AC (2017) Highly variable recurrence of tsunamis in the 7,400 years before the 2004 Indian Ocean tsunami. Nature Communications 16019 doi:10.1038/ncomms16019

Shulgin A, Kopp H, Mueller C, Planert L (2011) Structural architecture of oceanic plateau subduction offshore Eastern Java and the potential implications for geohazards. Geophysical Journal International, pp 1228. doi: 10.1111/j.1365246X. 2010.04834.x

Synolakis C, Imamura F, Tsuji Y, Matsutomi H, Tinti S, Cook B, Chandra Y, Usman M (1995)

Damage, conditions of East Java tsunami of 1994 analyzed. EOS, Trans Am Geophys Union (76): pp. 257, 261–262

Titov VV, Moore CW, Greenslade DJ, Pattiaratchi C, Badal R, Synolakis CE et al (2011) New tool for inundation modeling: community modeling interface for tsunamis (ComMIT). Pure Appl Geophys 168:2121–2131

Titov VV, Kânoğlu U, Synolakis CE (2016) Development of MOST for real-time tsunami forecasting. Journal of Waterway, Port, Coastal, and Ocean Engineering, 142, 03116004. doi:10.1061/(ASCE)WW.1943-5460.0000357

Tregoning P, Brunner FK, Bock Y, Puntodewo SSO, McCaffrey R, Genrich J, Calais E, Rais J, Subarya C (1994) First geodetic measurement of convergence across the Java Trench. Geophys. Res. Lett , vol 21 (19), pp 2135–2138

Tsuboi S (2000) Application of Mwp to tsunami earthquake, Geophys. Res. Lett., 27, 3105–3108, doi:10.1029/2000GL011735

Tsuji Y, Imamura F, Matsutomi H, Synolakis CE, Nanang PT, Jumadi Harada S, Han SS, Arai K, Cook B (1995) Field survey of the East Java earthquake and tsunami of 3 June 1994, Pure Appl. Geophys. 144, 839-854

Wells D, Copperfield K, (1994) New Empirical Relationships among Magnitude, Rupture Length, Rupture Width, Rupture Area, and Surface Displacement. Bulletin of the Seismological Society of America, vol 84, pp 9741002

Wichmann CEA (1918) Die Erdbeben des Indishen Archipels Bis Zum Johpe 1857, (in Dutch), Koninkl. Nederlandse Akad. Wetensch. Verh. 2nd Sect. 20, 193 p

Wichmann CEA (1922) Die Erdbeben des Indischen Archipels von 1858 bis 1877, (in Dutch) Amsterdam: Konink. Nederlandse Akad. Wetensch. Verh. 2nd Sect. 22, 209 p

WorldPop Archive Browser - File group listing: http://www.worldpop.org.uk/data/files/index.php?dataset=161&action=group, 2020 data last access: 23 Aug 2017.

Young RW, Bryant EA, Price DM (1996) Catastrophic wave (tsunami?) transport of boulders in southern New South Wales, Australia, Zeitschrift für Geomorphologie N.F. 40, 191–207